

Validation of Hybrid Tracker Concept

October 11, 2002

**Prepared for
NASA Ames Research Center
Moffett Field, California**

**Prepared by
Edwin D. McConkey**

**Science Applications International Corporation
Arlington, Virginia**

Work Performed Under Contract No. NAS2-98002

Task Order 68

Sub-task 2

Table of Contents

Introduction	1
Background.....	1
Tasking – Hybrid Radar Filter Concepts	1
Task Requirements	2
Data Sources	2
Study Methodology.....	4
The PID Controller	4
Filter Gain Constants	6
Analysis - Ground Speed and Track Angle Estimation	7
Flight Data Inputs	7
PID Estimator Data Analysis.....	8
Statistical Analysis of the PID Estimator	9
Summary Analysis of the PID Estimator.....	9
Hybrid Filter – “Detect Turn and Coast” Concept	9
Performance of the Hybrid Filters over the Duration of Flight 728	11
Detailed Performance of the Hybrid Filters for Segments of Flight 728.....	13
Application of Filter Concepts to Post-Flight Track Adherence Determination	14
Analysis – Post-Flight Determination of Track Adherence.....	16
Track Adherence in Straight Flight Segments.....	16
Track Adherence at Turn Points	16
Track Adherence – Angle Bisector Methodology	17
Track Adherence – Curved Segment Methodology	18
Track Angle Identification and Delay Correction	18
Conclusions and Recommendations	21
Conclusions – Application of the Hybrid Filter Concept to Velocity Estimation for DST’s	21
Conclusions – Application of the Hybrid Filter Concept for Post-Flight Track Adherence Determination.....	21
Recommendations.....	22
References	23
Acronyms	24

List of Figures

Figure 1	Number and Distribution of Turns for Flight 728	25
Figure 2	Radar Flight Track of Flight 728.....	26
Figure 3	GPS Flight Track of Flight 728.....	27
Figure 4	Radar Flight Track for Small Segment of Flight 728.....	28
Figure 5	GPS Flight Track for Small Segment of Flight 728.....	29
Figure 6	Unusual Data Points for Flight 728 Occurring at Time = 68285 Seconds.....	30
Figure 7	Comparison of Ground Speed for Radar and PID Tracker for First Half of Flight 728 (TC = 20 seconds, TCV = 50 seconds).....	31
Figure 8	Comparison of Ground Speed for Radar and PID Tracker for Second Half of Flight 728 (TC = 20 seconds, TCV = 50 seconds).....	32
Figure 9	Comparison of Track Angle for Radar and PID Tracker for First Half of Flight 728 (TC = 20 seconds, TCV = 50 seconds).....	33
Figure 10	Comparison of Track Angle for Radar and PID Tracker for Second Half of Flight 728 (TC = 20 seconds, TCV = 50 seconds).....	34
Figure 11	Comparison of Ground Speed for Radar and PID Tracker for First Half of Flight 728 (TC = 40 seconds, TCV = 100 seconds).....	35
Figure 12	Comparison of Ground Speed for Radar and Hybrid Tracker for Second Half of Flight 728 (TC = 40 seconds, TCV = 100 seconds).....	36
Figure 13	Comparison of Track Angle for Radar and Hybrid Tracker for First Half of Flight 728 (TC = 40 seconds, TCV = 100 seconds)	37
Figure 14	Comparison of Track Angle for Radar and Hybrid Tracker for Second Half of Flight 728 (TC = 40 seconds, TCV = 100 seconds)	38
Figure 15	“Detect Turn and Coast” Hybrid Filter Using Radar Ground Speed for First Half of Flight 728	39
Figure 16	“Detect Turn and Coast” Hybrid Filter Using Radar Ground Speed for Second Half of Flight 728.....	40
Figure 17	“Detect Turn and Coast” Hybrid Filter Using PID Ground Speed for First Half of Flight 728	41
Figure 18	“Detect Turn and Coast” Hybrid Filter Using PID Ground Speed for Second Half of Flight 728.....	42
Figure 19	“Detect Turn and Coast” Hybrid Filter Using Radar Ground Speed for Flight Segment 728-2.....	43
Figure 20	“Detect Turn and Coast” Hybrid Filter Using Radar Ground Speed for Flight Segment 728-3.....	44
Figure 21	“Detect Turn and Coast” Hybrid Filter Using PID Ground Speed for Flight Segment 728-2.....	45
Figure 22	“Detect Turn and Coast” Hybrid Filter Using PID Ground Speed for Flight Segment 728-3.....	46
Figure 23	“Detect Turn and Coast” Hybrid Filter Using Radar Ground Speed for Flight Segment “Turn 5 and 6”	47
Figure 24	“Detect Turn and Coast” Hybrid Filter Using Radar Ground Speed for Flight Segment “Turn 7 and 8”	48
Figure 25	“Detect Turn and Coast” Hybrid Filter Using Radar Ground Speed for Flight Segment “Long Coast”	49

Figure 26 Correlation of GPS Track Angle and Track Angle from PID Estimator (TC = 20 seconds)	50
Figure 27 GPS Track Angle and Time-Shifted PID Track Angle – First Half of Flight 728.....	51
Figure 28 GPS Track Angle and Time-Shifted PID Track Angle – Second Half of Flight 728 ..	52
Figure 29 Error in Time-Shifted PID Track Angle – First Half of Flight 728	53
Figure 30 Error in Time-Shifted PID Track Angle – Second Half of Flight 728.....	54
Figure 31 Comparison of GPS Turn Indicator and PID Turn Indicator for First Part of Flight 728	55
Figure 32 Comparison of GPS Turn Indicator and PID Turn Indicator for Second Part of Flight 728	56
Figure 33 Comparison of GPS Turn Indicator and PID Turn Indicator for Third Part of Flight 728	57

List of Diagrams

Diagram 1 PID Estimator Block Diagram.....	5
Diagram 2 Track Adherence during Straight Segments of a Flight.....	16
Diagram 3 Cross Track Error Determination During a Turn.....	17

List of Tables

Table 1 Ground Speed and Track Angle Error Statistics for PID Estimator and Radar Tracker ...	9
Table 2 Statistical Comparison of Unfiltered and Filtered Ground Speed Errors for the Duration of Flight 728.....	12
Table 3 Statistical Assessment of DT&C-R Hybrid Filter Performance	15
Table 4 Statistical Assessment of TD&C-P Hybrid Filter Performance	15
Table 5 Inherent Cross Track Error at Turn Points Caused by Use of the Angle Bisector Methodology (Turn Radius = 7 NM).....	18
Table 6 Error in Time-Shifted Track Angle Output of PID Estimator (TC = 20 seconds)	19

Introduction

Since 1989, the National Aeronautics and Space Administration (NASA) has been developing elements of the Center-Terminal Radar Control (TRACON) Automation System (CTAS). CTAS provides a broad array of Decision Support Tools (DST's) that assist controllers in performing a variety of air traffic control (ATC) functions. A key function of CTAS is to model aircraft trajectories to allow predictions of future aircraft positions to assist controllers in efficiently and effectively managing air traffic within their jurisdiction. A key issue in CTAS development is the accuracy of the CTAS modeling function.

Two flight demonstrations were conducted (Phase I in October 1992 and Phase II in September 1994) to evaluate CTAS accuracy during the en route arrival phase of flight. The Transport System Research Vehicle (TSRV) Boeing 737 Model 100 aircraft, based at NASA Langley Research Center, flew a combined total of 57 arrival trajectories during these demonstrations.

These flights were tracked by radar using the Federal Aviation Administration's (FAA's) Host Computer System located at the Denver Air Route Traffic Control Center (ARTCC). In addition, position and velocity information from the aircraft's differential Global Positioning System (GPS) were recorded during these flights. The GPS information is very accurate and is available at approximately one-second increments for the duration of the flight. This allows the use of the GPS information for providing the true position and velocity of the aircraft during the flight. For the work described herein, the radar information was processed and time correlated with the GPS data to assess the performance of the radar processing techniques.

Background

Error in the FAA Host tracker contributes to trajectory prediction uncertainty. Field tests have indicated that the most significant component of Host tracker error is velocity. Transient errors of up to 150 knots are common during maneuvers. Previous efforts to filter Host data for DST applications have failed to significantly reduce these transient effects. Data from two time periods are available for this analysis, 1992 and 1994. Each data set contains cruise and descent segments. From the 1992 TSRV flights there are 20 runs of approximately 15 minutes each. These data have with no turns during the en route descents. From the 1994 TSRV flights there are approximately 20 hours of flight data gathered over 6 flights. These flights contain data from all phases of flight and include turns.

The FAA's William J. Hughes Technical Center (WJHTC) is independently assessing radar tracker performance analysis in terms of its impact on the accuracy of emerging Air Traffic Management (ATM) DST technologies such as CTAS and User Request Evaluation Tool (URET). The FAA has expressed interest in NASA's field test data/results as a contributing source of data for their studies.

Tasking – Hybrid Radar Filter Concepts

Objectives: The initial objective of this sub-task is to develop and validate linear and non-linear filter concepts (described herein as hybrid trackers) based on a combination of modern techniques [1] and discrete modes dependent on observed aircraft state (e.g., straight and level, in turn, post-turn, climb, and descent). A second objective of the work described herein is to translate NASA results into a format of use to the FAA and extend the analysis methodology to make the results relevant to the FAA's studies.

Tasking: Previous analysis and assessments have characterized tracker ground speed estimation errors for the following maneuvers: accelerations, decelerations, ascents, descents, and straight-and-level flight that are detectable from tracker observations [1]. The purpose of this effort is to complete the analysis of velocity estimation errors for turn maneuvers. This effort will use the approximately 20 hours of flight and tracker data collected during the 1994 TSRV field test. The initial requirement of this task is to develop a hybrid tracker-velocity filter using a combination of modern filtering techniques (e.g., as detailed in [1]) and discrete modes dependent on aircraft state observed from tracker data. This task shall include analysis and testing to validate the hybrid filter concept.

A second requirement of this task is to adapt the results of this work and perform supporting trajectory analysis to provide the FAA with results in the format needed to support the FAA analyses. This task shall define the format necessary and provide the FAA with the data electronically along with a textual description documenting the characteristics and source of data from the NASA field tests.

Task Requirements

Meetings were held with NASA and FAA personnel to clarify and finalize task requirements. The NASA portion of the task was quite straightforward. Using modern state estimation techniques and discrete modes of flight that could be deduced from radar data, linear and non-linear estimation techniques were to be synthesized with a goal of improving ground speed estimation, particularly during turns. Data from the NASA flight demonstrations in Denver in the mid-1990s were to be used to evaluate the performance of these estimation techniques. The key performance metric was the reduction of tracker ground speed errors during turns. The NASA requirement for ground speed data occurs in real time. This means that only information obtained from the FAA's Host Computer system is available to calculate the required ground speed estimates.

For the FAA portion of the task, it was necessary to review the work performed for the NASA effort and explore areas where this work could be useful to the FAA office at WJHTC. From this review, it was found that one of the requirements of the FAA was to assess adherence to flight plan of aircraft operating in the National Airspace System (NAS). There are a variety of reasons that aircraft deviate from their flight plan. These include tactical deviations for weather avoidance, directions from ATC for spacing and/or separation assurance, and rerouting due to delays or other problems at downstream sectors or the destination airport. From radar tracker data, the FAA WJHTC office performs post-flight data analysis on samples of flights to assess adherence to flight plan. Since these analyses are performed post flight, the data processing technique can make use of delay compensation techniques to mitigate negative aspects of heavy filtering. These techniques may include time shifts to compensate for fixed delays.

Data Sources

Two sources of data were available to support this project. The first data source was radar data from the output of the FAA's Host tracker. These data are output at intervals of approximately 12 seconds, which is the nominal sweep rate of the FAA's en route radar system. The radar data files contain the following key parameters:

- X, Y – position of the aircraft measured in the local Denver stereographic projection coordinates (units are in Nautical Miles (NM))
- Alt – Mode C altitude of the aircraft in 100's of feet
- Bcst_GS – Ground speed of the aircraft (knots)
- Vert_Spd – Vertical speed of the aircraft (feet/minute)
- Time – Time (measured in seconds) of the data record (measured in Universal Coordinated Time (UTC))
(Note: The data file has a time record in the file header. The time of each data record is the elapsed time in seconds measured from the time of the header record)

GPS data were recorded approximately once per second throughout the duration of the flight. Occasionally there were gaps in the data that lasted between 1 and 64 seconds. Small gaps (less than 10 seconds) were filled with interpolated data to allow easy time-merging of GPS and hybrid tracker data records. GPS data files contain the following key parameters:

- X, Y – position of the aircraft derived from the aircraft's latitude and longitude transformed into local Denver stereographic projection coordinates (units are in NM)
- Alt – Altitude of the aircraft derived from the aircraft's GPS altitude transformed into altitude above mean sea level (MSL)
- Vgnd – Ground speed of the aircraft derived from GPS (knots)
- Course – Ground track of the aircraft derived from GPS (measured in degrees from true North)
- dalt_dt – Rate of climb/descent of the aircraft derived from GPS (feet/minute)
- Time – Time of the GPS record (measured in seconds of the day in UTC coordinates)

The radar tracker and GPS data sets have common units and reference systems. This allows direct comparison of data records without conversion of units.

Study Methodology

Reference 1 describes state estimation techniques and the use of these techniques for predicting the future state of aircraft in flight. The aircraft states are the horizontal components of the aircraft position, ground speed, and track angle. Three types of state estimation techniques are discussed. Each of these techniques can be applied to the hybrid tracker concept. These systems are the Kalman Filter, the Estimator Using Inverse Model, and the Hybrid Estimator.

The Kalman Filter is based on linear feedback control theory. It provides for continuous measurement of the error covariance, which allows gain coefficients in the feedback loop to be set based on the error covariance. It provides for direct estimation of the horizontal position, ground speed and track angle.

The Estimator Using Inverse Model uses a controller based on classical control theory as its basis. The estimator uses a Proportional-Integral-Derivative (PID) controller to estimate the horizontal position coordinates. The estimator is used in conjunction with low-pass filters to smooth velocity and track information emanating from the controller to provide outputs of these states. This estimation technique uses fixed gains in the feedback loop and provides consistent performance in terms of processing delays.

The Hybrid Estimator uses statistical estimation techniques to measure horizontal component velocities. Aircraft state estimation is determined from the estimates of these component velocities. It was found in [1] that some of the velocity estimates were quite noisy. It was then determined that smoothing the velocity estimates using a low-pass filter provide improved performance. This estimator then becomes a combination of statistical estimation plus linear filtering. For this reason it is described as a Hybrid Estimator.

The estimation process has two major considerations. The first consideration is the requirement to smooth (or filter) data to reduce noise. The second consideration is the delay encountered due to the need to filter. These two considerations are typically at odds with each other. A greater degree of filtering causes greater delays. With the Kalman Filter, gains are set according to the error covariance values that are measured during the estimation process. These gains, and therefore the delays, are not constant over the duration of the flight. With the PID estimator, the gains are fixed according to a priori estimates of the degree of filtering required. These fixed gains produce fixed delays in the estimator outputs.

Initial efforts were directed at using the Kalman Filter and PID Controller techniques. During this time, it was learned that a key FAA requirement for tracker data involved post-flight analysis of radar data to assess performance of flights in achieving adherence to flight plans. The Kalman Filter and PID Controller estimation techniques were assessed as to their ability to perform the velocity estimation functions required by NASA and flight plan adherence analysis by WJHTC. It was determined that, because of the fixed nature of delays, the PID estimator was the better choice for detailed analysis to be applied to the combined requirements of NASA and the FAA. For this reason, major emphasis for the analysis involved development, analysis and testing of the PID Controller state estimation method.

The PID Controller

The PID Controller shown in Diagram 1 was developed to investigate the NASA and FAA applications. There are some differences from the PID Controller presented in [1]. A principal difference involves the low-pass filtering of the rate information. In [1], the X

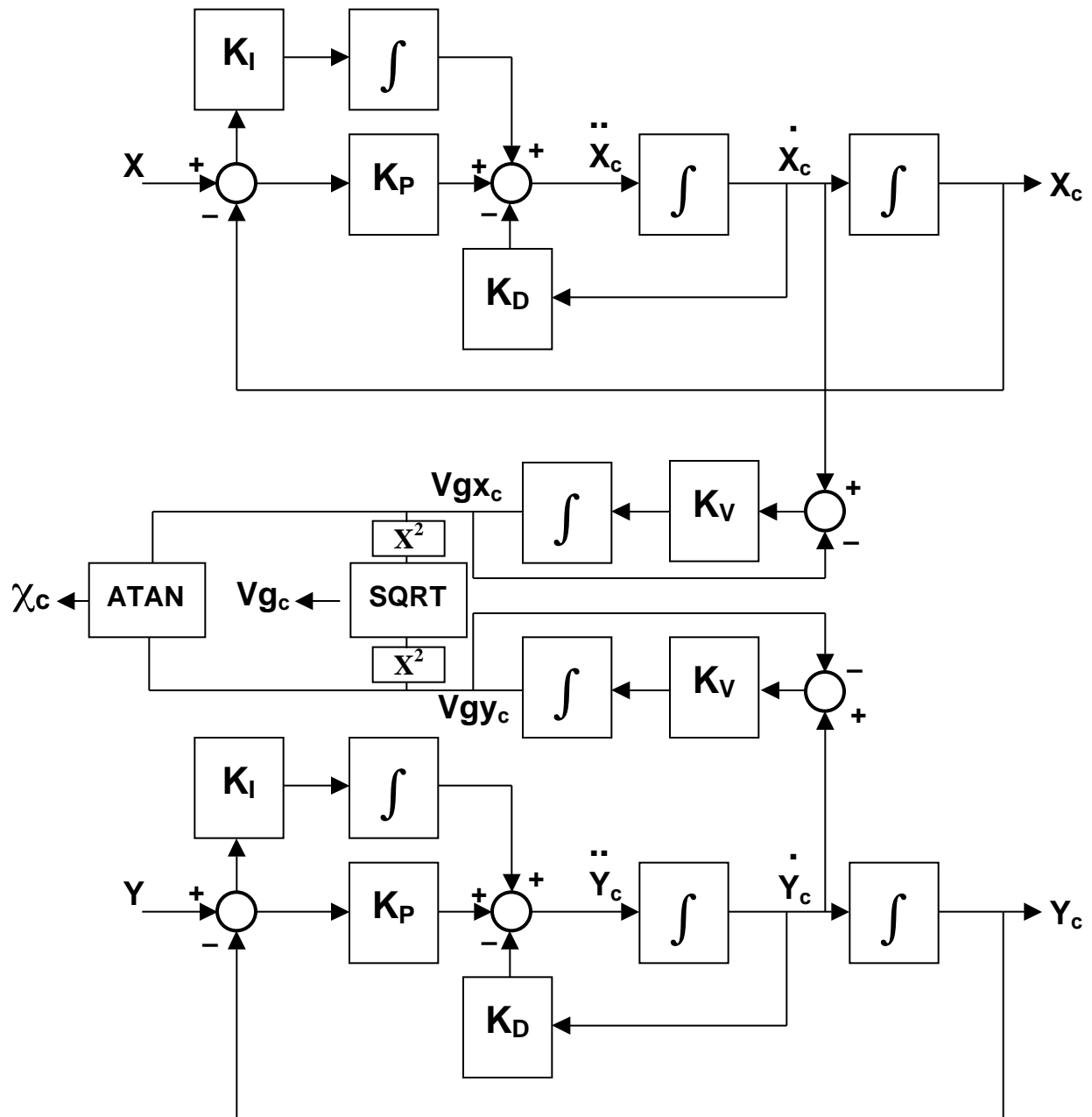


Diagram 1 PID Estimator Block Diagram

and Y component velocities are first passed through a non-linear process to determine ground speed and track angle. Then these quantities are passed through the low-pass filters with gains set appropriately for the characteristics of the ground speed and track angle. It was found with the TSRV flights, the aircraft flew through many circuits in a repeating pattern. Because of these many circuits, the track angle went through many transitions of the non-linear boundary between 360 degrees and 0 degrees. As a means of eliminating this non-linear transition, the implementation in Diagram 1 performs the non-linear transformation from component velocities to ground speed and track angle after the low-pass filtering function has been performed. This eliminates the non-linear transitions, but has the drawback of being unable to use separate filter constants for ground speed and track angle.

A second difference in the PID Controller in Diagram 1 and the PID controller in [1] involves the velocity feedback loop. In [1, Figure 4], the ground speed and track angle are resolved into component velocities and fed back with gain K_D into the PID estimator at the point prior to the second integrator (at the second summation node). This was tested in the PID Controller shown in Diagram 1 and it was found that the delays introduced by the low-pass filters caused stability problems with the PID Controller. To eliminate these stability problems, the feedback configuration shown in [1, Figure 4] was used. In this implementation, the velocity signal from within the PID Controller is fed back with gain K_D to the node described above. This configuration eliminated the stability problem.

Filter Gain Constants

The PID estimator has four gain values (K_I , K_P , K_D and K_V) that must be assigned. Reference 1 suggests that three of the four gains can be established by equating the coefficients to the Butterworth form using the *integral of time multiplied by the absolute value of error* (ITAE) with zero ramp error criterion described in Reference 2. For the PID implementation, which has a third order polynomial in the denominator of the transfer function, the relationship between the gains is associated with the characteristic frequency of the filter (identified as ω_0) by the following formulas:

$$\begin{aligned} K_D &= 1.75 \times \omega_0 \\ K_P &= 3.25 \times \omega_0^2 \\ K_I &= \omega_0^3 \\ TC &= 1 / \omega_0 \end{aligned}$$

The units of ω_0 are in terms of reciprocal seconds. Hence, the term $1 / \omega_0$ has units of time and is associated with the time constant (TC) of the estimator. The parameter TC is used in the analysis sections of this report to identify the various PID filter settings.

Similarly, the gain of the low pass filter, K_V , has units of reciprocal time and its value is established by setting its reciprocal value, TC_V ,

$$\text{where } TC_V = 1 / K_V.$$

Analysis – Ground Speed and Track Angle Estimation

The PID Estimator shown in Diagram 1 was designed and implemented in a computer program using Microsoft QuickBasic software. A second-order Runge-Kutta integration method was employed. The time step for integration was set at 1 second. The radar position coordinates (X and Y) are available at 12-second intervals (or an integer multiple of 12 seconds if a radar position update is missed). In the early configuration of the PID estimator development, a “sample and hold” technique was used for the radar position inputs. A refinement to this technique was developed to improve the estimation process. The refinement provides an update to the radar position based on the velocity and track outputs of the filter. To implement this, the ground speed output of the estimator is separated into X and Y components by multiplying by the sine or cosine of the track angle. At each time step, the input data stream for X and Y is tested to see if a new radar position is available. If so, the updated position is used by the PID estimator and the elapsed time since the last update is reset to zero. If no new radar position is available, the estimated change in radar position from the last radar update ($_X_R$, $_Y_R$) is estimated by multiplying the elapsed time since the last update ($_T_R$) by the appropriate component velocity (VG_x , VG_y). This produces $_X_R = _T_R \times VG_x$ and $_Y_R = _T_R \times VG_y$. The radar position is updated each time step by adding the estimated change to each component ($X + _X_R$, $Y + _Y_R$).

Flight Data Inputs

Flight 728, flown on September 16, 1994, was used as the principal test case. This flight provided a broad range of climbs, descents, and turns for evaluating the tracking filters that were developed during the task. The flight lasted approximately 2 hours and 40 minutes. The aircraft flew multiple circuits of the test area northwest of Denver and contained 21 turns ranging from 10 degrees to 360 degrees. The flight also had 3 descents from Flight Level (FL) 330 to 17,000 feet MSL for the En Route Descent Advisor (EDA) evaluation. Two of the descents were followed by climbs back to FL 330.

This flight was conducted for research purposes. As such, it follows a prescribed flight plan only during segments of the flight when data was being collected for the en route descents. During other times during the flight, the aircraft was either being repositioned to begin another en route descent, to perform some other research function, or to return to the airport. For this reason, this flight and other flights conducted during the flight demonstration are not typical of commercial flights flown in the NAS.

Figure 1 shows the magnitude and distribution of the turns. Figure 2 shows the radar flight track for Flight 728. Time marks are shown in the ground track to indicate the progress of the aircraft. Figure 3 shows the GPS flight track and time marks for the same flight. Figures 4 and 5 show radar and GPS tracks for a small segment of the flight, a 360-degree turn late in the flight. Comparing Figures 4 and 5, the errors in the radar track tend to produce a rather ragged track, while the highly accurate GPS data exhibits a smooth track for the same flight segment.

Figure 6 shows an unusual occurrence during the flight where the radar data indicates that the aircraft reversed its course between data points. This may have occurred at a point where there is an overlap in coverage from two radars. At such points, the Host system uses a process described as mosaicing to assemble the separate radar data points into a single data set. Differences in the two radar data sets at these interfaces could produce unusual data points as shown in Figure 6.

PID Estimator Data Analysis

The X and Y data from the radar files for Flight Number 728 were used as input to the PID Estimator program. State variable outputs were X and Y position, ground speed (V_G) and track angle with respect to True North (τ). The latter two state variables, V_G and τ , were of primary interest in this study.

Several program runs were made using different time constants for the PID loop and the low-pass component velocity filter. The resulting graphs for V_G and τ were inspected to assess the filter performance in terms of smoothing and delay.

Figures 7 and 8 compare the PID Estimator output for V_G (green line) with the radar tracker ground speed (blue line) and the GPS ground speed (brown line). Figure 7 shows the first half and Figure 8 the second half of the flight. To identify flight turn points, the magenta line in the upper part of the graph shows when the GPS system indicated a turn rate in excess of 30 degrees per minute. A “1” indicates a turn and a “0” indicates no turn. This scale is shown on the vertical axis on the right side of the graph. In this run the time constants were set at 20 seconds for TC and 50 seconds for TC_V . It is apparent from Figures 7 and 8 that the PID Estimator outputs for ground speed are not sufficiently filtered to produce a smooth output. Both the PID Estimator and the radar show difficulty in tracking the ground speed at the turn points. For instance, at the turn near the time of 64000 seconds, GPS has a ground speed of 425 knots. The PID Estimator output dips to 370 knots and the radar tracker dips to 290 knots. Similar errors are apparent at times of 64900 seconds, 67100 seconds, 68300 seconds, and 69800 seconds. Note that the error at 68300 seconds occurs at the unusual radar data points noted in Figure 6.

Figures 9 and 10 compare results for the track angle measurements for the filter constants identified in the previous paragraph. The track angle output of the PID Estimator shows close agreement with the GPS track angle, but with some delay. The one area where the hybrid track angle output differs significantly from GPS is the region around 68,300 seconds. This problem is due to the unusual radar data points in this area shown in Figure 6 and is not considered to be a limitation of the PID Estimator. Measurements of this delay indicate that the PID Estimator output is delayed by 54 seconds from the GPS track angle output. The PID Estimator output shows adequate filtering for the track angle measurement. This is in contrast with the ground speed output, which does not have adequate filtering with these time constants.

To improve the ground speed filtering, the time constants were increased to $TC = 40$ seconds and $TC_V = 100$ seconds. Figures 11 and 12 show the PID Estimator ground speed during the first and second half of the flight. With these time constants the ground speed output becomes much smoother than with the smaller time constants represented in Figures 7 and 8. However, the velocity output of the PID Estimator exhibits undesirable characteristics at the turn points similar to the output of the FAA’s Host Tracker. For example, at Time = 64,000 seconds, both the radar and the PID Estimator output dip to a ground speed of 300 knots, while the GPS shows a ground speed of 425 knots. Clearly the increased time constants of the PID Estimator have improved the smoothness of the ground speed output, but at the expense of performance at the turn points.

Figures 13 and 14 present the track angle output of the PID Estimator with the time constants described in the previous paragraph. These graphs indicate an increase in the delay and slow response to changes in the track angle. These graphs indicate poorer performance for the track angle output using the larger time constants. Measurement of delay shown in Figures 13 and 14 was approximately 94 seconds.

Statistical Analysis of the PID Estimator

Ground speed and track angle errors for the FAA’s radar tracker and the PID Estimator were calculated. The GPS ground speed (or track angle) was subtracted from the outputs of the radar tracker and the PID Estimator. The results are time series of PID Estimator and radar tracker errors for the duration of the flight. Error statistics (mean and standard deviation) were calculated for each of the time series. The results are shown in Table 1.

Table 1 Ground Speed and Track Angle Error Statistics for PID Estimator and Radar Tracker

	PID Estimator (TC = 20 sec) (knots)	PID Estimator (TC = 40 sec) (knots)	Radar (knots)
Ground Speed Error			
Mean	-8.4	-29.0	-23.4
Standard Deviation	42.6	50.0	49.9
Track Angle Error	(degrees)	(degrees)	(degrees)
Mean	-10.7	-19.1	-4.4
Standard Deviation	24.6	36.5	14.5

The statistics shown in Table 1 indicate that increasing the PID Estimator time constants causes the mean error to increase. This is largely due to the increased delay incurred with larger time constants. The statistics also indicate that the ground speed statistics for the radar are similar to those of the PID Estimator with the 40-second time constant. For the track angle errors, the statistics for the FAA’s radar tracker show smaller errors than for either of the PID estimator cases.

Summary Analysis of PID Estimator

The PID Estimator was able to reduce high frequency errors and produce smooth outputs of ground speed and track angle. However, this smoothing comes at the expense of delay or latency in the PID Estimator outputs. These delays tend to increase the mean errors observed in comparison to the GPS ground speed and track angle outputs. The track angle output of the PID Estimator with the 20-second time constant appears to produce a good replication of the GPS track angle, albeit delayed by about 54 seconds. The track angle output with the 40-second time constant indicated excessive filtering resulting in sluggish response. The ground speed output of the PID Estimator with the 20-second time constant contains high frequency noise that indicates that filtering is not adequate. The ground speed output with the 40-second time constant produces a smooth output. However, this output shows large error characteristics at turn points in the flight path. These errors are similar to those observed in the radar ground speed output. The ground speed output of the PID Estimator did not demonstrate any substantial improvement in performance over that of the FAA’s radar tracker.

Hybrid Filter – “Detect Turn and Coast” Concept

Because the ground speed estimates of the FAA’s radar tracker and the PID Estimator deteriorate at route turn points, it is natural to investigate the use of discrete modes such as turn detection and climb/descent detection in an attempt to improve the ground speed performance of radar trackers or other estimation techniques. The results of the analysis of the PID Estimator

indicated that it performed quite well as a turn indicator, but with some delay in detection. Using these results, a hybrid filter concept was developed, which is identified as the ‘Detect Turn and Coast’ (DT&C) concept. The hybrid filter makes use of the PID Estimator for turn detection. Once a turn is detected, the ground speed output is allowed to “coast” at some predetermined value until the turn has been completed. At this point, the ground speed output is then switched back to the original source of ground speed information. The logic applied in the development of the filter is described in the following paragraph.

The PID Estimator with a 20-second time constant was used to detect the beginning of a turn. A turn rate exceeding 30 degrees/minute was used as the threshold for identifying the start of the turn. When the turn rate fell below 30 degrees/minute the turn was considered completed. The delay caused by using the PID Estimator is 54 seconds. Therefore, a ground speed estimate measured 54 seconds prior to the detection of the turn will not be contaminated with the dynamics of the turn. When a turn is detected, the ground speed output is switched from its level flight source to a saved value of ground speed measured 54 seconds prior to the switch. The hybrid filter holds this value of ground speed until a specified time after turn has been completed.

The specified time after turn completion was set empirically by analysis of the performance of the filter as applied to Flight 728. Initially, this point was set to be at the point where the PID Estimator indicated that the turn was complete. Because of the delay in the PID Estimator, this means that the ground speed is switched back to its original source 54 seconds after the actual turn has been completed. Inspection of this logic indicated that this switch point was occurring too early. Remnants of the turn error were still evident when the ground speed switched back. Additional delay was added before returning the ground speed to its original source. The final value of added delay was also set at 54 seconds. This value was selected based on performance at five significant ground speed error “spikes.” These spikes occurred at 64000, 64900, 67100, 68200, and 69900 seconds. The use of 54 seconds for this additional delay is a coincidence and not related to the 54-second delay caused by the PID Estimator.

Two sources of ground speed information were used in evaluating the DT&C concept – radar tracker (identified as DT&C-R) and PID Estimator with the 40-second time constant (identified as DT&C-P). The results of applying this hybrid filter logic are presented in Figures 15 through 25. These figures are quite complex so some explanation of their content is provided herein.

The graph is divided into two sections. The upper section corresponds to the axis coordinates on the right side of the page. These coordinates range from -1 to +1 and indicate discrete modes related to turning flight, climbs and descents. The magenta line identifies times that GPS indicates a turn. If GPS indicates a turn rate of 30 degrees/minute or more, the GPS turn indicator has value of +1. If GPS indicates a turn rate of less than 30 degrees/minute, the GPS turn indicator has value of 0.

The purple line identifies times that the PID Estimator (with a time constant of 20 seconds) indicates a turn. If the PID Estimator indicates a turn rate of 30 degrees/minute or more, the PID turn indicator has value of -1 (to distinguish it from the GPS indicator). If the PID Estimator indicates a turn rate of less than 30 degrees/minute, the PID turn indicator has value of 0.

The orange line identifies times that the aircraft is climbing, level, or descending. This indicator is driven by passing the Mode-C altitude from the FAA’s radar system through a low pass filter

with a time constant of 40 seconds. If the climb rate is greater than or equal to 500 feet/minute, the indicator has value +0.5 indicating a climb. If the climb rate is less than or equal to -1000 feet/minute, the indicator has value of -0.5 indicating a descent. Otherwise, the indicator has value 0 to indicate level flight.

The lower part of the graph presents a time history of ground speed derived from several sources. The ground speed values are shown on the axis on the left side of the graph. GPS ground speed is used as the “truth system,” and is shown by the blue line on all graphs.

In Figures 15 through 18, either FAA radar or PID ground speed (but not both) is shown. Depending on the source of ground speed information used in the case being studied, the green line represents either ground speed from the FAA’s radar system or from the PID Estimator (with a time constant of 40 seconds). Similarly, the brown line indicates the output of the DT&C hybrid filter for the corresponding source of ground speed information (DT&C-R for FAA radar or DT&C-P for the PID Estimator).

In Figures 19 through 25, both the ground speed from the FAA’s radar and the PID estimator are shown. The green line shows the radar ground speed and the red-orange line shows the PID ground speed. The blue-gray line shows the DT&C-R filter output derived from radar ground speed in Figures 19, 20, 23, 24, and 25. In Figures 21 and 22, the blue-gray line shows the DT&C-P filter output derived from the PID Estimator ground speed.

Performance of the Hybrid Filters over the Duration of Flight 728

Figure 15 shows the DT&C-R concept applied to the first half of Flight 728. The FAA’s radar is used as the source of ground speed in this graph. Initially the DT&C-R filter triggers the coast mode* during the turn when the aircraft is climbing to altitude. At this time it holds a ground speed value that is lower than the GPS ground speed and the radar ground speed. During the turn at the end of climb (62800 seconds), the filter holds a ground speed that evens out the variations shown in the radar ground speed. At 64000 seconds the hybrid filter significantly reduces the large negative spike in radar ground speed by holding a value of slightly greater than 450 knots. Similar improvement is shown at 64850 seconds by eliminating the negative spike in radar ground speed. At 65400 seconds the en route descent identified as 728-2 begins. The GPS ground speed shows a large negative swing followed by a large positive increase at the end of the descent. Neither the radar nor the DT&C-R filter output perform well during this descent and climb out. The performance of the filter for the two en route descents, 728-2 and 728-3, are discussed in more detail in later paragraphs.

Figure 16 shows the DT&C-R concept applied to the second half of Flight 728. Good filter performance is shown during the level turns near 67000 seconds. The filter effectively corrects the large, negative ground speed spike that occurs at this time. The second en route descent, 728-3, occurs at about 67850 seconds. The filter does not perform well during the turn in this descent run. It holds a value that is high by more than 50 knots. Later in the flight, the filter corrects negative spikes at 69100 seconds (at the end of a climb) and 69800 seconds (during level flight).

* Note that for both the DT&C-R and the DT&C-P configurations, the ground speed coast period is triggered by the turn rate, which is calculated by the PID Estimator with the 20-second time constant. For this reason, the coast periods for the two hybrid filters are identical. The only difference is the source of ground speed information – radar or PID Estimator using the 40-second time constant.

Figure 17 shows the DT&C-P hybrid filter, using ground speed from the PID estimator, applied to the first half of Flight 728. The coast period of the DT&C-P filter is triggered during the turn during climb out. As during the radar ground speed case, the filter holds a ground speed value that is significantly lower than the GPS ground speed. During the turn at the end of climb out (62800 seconds), the filter holds a ground speed that corrects a negative spike, but the filter does not coast long enough. This causes a downward spike in the filter ground speed output just after 63000 seconds. This is evidence that the coast period should be set for a longer duration than 54 seconds. At 64000 seconds, the hybrid filter shows similar performance by eliminating the large negative spike by holding a value of slightly greater than 450 knots. However, again the filter does not coast long enough and a negative spike is observed near 64100 seconds. Similar performance is shown at 64850 seconds by eliminating much of the negative spike PID ground speed, but a large negative spike in hybrid filter ground speed is observed at 64950 seconds. During the en route descent 728-2 at 65400 seconds, DT&C-P filter holds a ground speed that is high by more than 50 knots. In the following climb, the filter holds a ground speed value that is low by about 40 knots (filter output is 360 knots while GPS ground speed is about 400 knots).

Figure 18 shows the DT&C-P hybrid filter using PID ground speed applied to the second half of Flight 728. Good filter performance is shown during the level turns near 67000 seconds. The filter effectively corrects the large, negative ground speed spike that occurs at this time. The second en route descent, 728-3 occurs beginning at about 67850 seconds. The filter shows similar poor performance observed during the descent 728-2, a value that is high by more than 50 knots. Later in the flight, the filter corrects negative spikes at 69200 seconds (at the end of a climb), but again it does not coast long enough to remove more of the error. At 69800 seconds (during level flight) the filter performs better than the PID ground speed, but the output is nearly 80 knots below the GPS ground speed.

The statistical performance of the DT&C-R and DT&C-P filters for the duration of Flight 728 was determined by comparing the outputs with the GPS derived ground speed. The results are shown in Table 2. The DT&C hybrid filter shows improved performance for both radar and PID ground speed sources. Overall, the DT&C-R filter (with the radar ground speed source) shows better performance than the filter with the PID ground speed source. For the radar case, the filter reduces the mean error by nearly 70 percent and reduces the standard deviation by 50 percent. The PID filter improvements were 53 percent for the mean error and 37 percent for the standard deviation.

Table 2 Statistical Comparison of Unfiltered and Filtered Ground Speed Errors for the Duration of Flight 728

Statistical Metric	----- Source of Ground Speed -----			
	Radar	DT&C-R (Radar)	PID Estimator (TC = 40 sec)	DT&C-P (PID)
Ground Speed Error	(knot)	(knots)	(knots)	(knots)
Mean	-23.4	-7.1	-29.0	-13.5
Standard Deviation	49.9	24.4	50.0	31.6

Detailed Performance of the Hybrid Filters for Segments of Flight 728

The results shown in Figures 15 through 18 are shown in greater detail for specific portions of Flight 728 in Figures 19 through 25. Figure 19 shows the DT&C-R performance during the en route descent identified as 728-2. The speed schedule used during this descent was a descent at constant Mach number (0.73) until reaching an indicated airspeed of 280 knots. Then the aircraft descended at 280 knots until an altitude of 17,000 feet MSL was reached. During the constant Mach portion of the descent, the true airspeed typically increases slightly because the outside air temperature increases at lower altitudes. If the winds are constant, this results in an increase in ground speed also. In Figure 19, an increase in GPS ground speed of about 15 knots is observed, which peaks at 450 knots at 65490 seconds. After this peak, the GPS ground speed diminishes to a value of 370 knots at bottom of descent. The GPS ground speed continues to descend until 65790 seconds when the airspeed begins to increase. The radar ground speed (green line) and the PID ground speed (orange line) show a slight increase followed by a decrease. However, the decrease shows a delay as compared to GPS. The radar ground speed tracks the GPS ground speed with a delay of about 25 seconds; the PID ground speed has a delay of about 60 seconds. The DT&C-R hybrid filter detects the turn 60 seconds after the GPS detects the turn. The hybrid filter then obtains the radar ground speed from 54 seconds prior (440 knots) and coasts using this ground speed value until 54 seconds after the PID Estimator indicates the turn is complete. Because of the decelerating descent, the hybrid ground speed is high throughout the coast period. The error is 44 knots high at the beginning of the coast period and 68 knots high at the end of the coast period.

Similar performance is shown in Figure 20 for the en route descent segment 728-3. For this descent the speed schedule is also a constant Mach number descent (0.73) with a transition to a constant indicated airspeed of 280 knots. The behavior of the GPS, radar, PID and DT&C-R hybrid filter are similar to those described for run 728-2. The output of the hybrid filter is 46 knots too high at the beginning of the coast period and 62 knots too high at the end of the coast period. The behavior during the two en route descents together with the physical explanation of the delays encountered with the radar and PID Estimator suggests that DT&C hybrid filter in its current configuration does not remedy ground speed errors observed during descents. The hybrid filter actually exacerbates the problem during climb and descent.

Figures 21 and 22 show the performance of the DT&C-P hybrid filter for the en route descent runs 728-2 and 728-3. The performance of this filter configuration parallels the DT&C-R filter. In the case of 728-2, the filter output is 47 knots too high at the beginning of the coast period and 71 knots too high at the end of the coast period. For run 728-3, the DT&C-P hybrid filter is 40 knots too high at the beginning of the coast period and 57 knots too high at the end of the coast period.

Figure 23 shows the performance of the DT&C-R filter for a portion of Flight 728 identified as Turns 5 and 6. This route segment is flown in the vicinity of the en route descents identified at 728-2 and 728-3. The graph begins during level flight at 63600 seconds. A descent begins at 63660 seconds and lasts until 63805 seconds. GPS detects a turn of 69 degrees at 63778 seconds, which occurs before the end of the descent. The aircraft levels off halfway through the turn. A second turn of 90 degrees begins at 63866. During the descent the GPS ground speed climbs from 430 knots to 475 knots. The GPS ground speed then falls back to 430 knots at the end of the descent and slowly falls to 410 knots at the end of the flight segment. The radar and PID Estimator respond to the increasing ground speed showing an increase to 450 and 460 knots

respectively. However, in response to the two turns, the radar ground speed falls to 295 knots at 63970 seconds and the ground speed from the PID Estimator falls to 300 knots at 64000 seconds. The DT&C-R filter is triggered to coast mode by the 69-degree turn at 63830 seconds holding the ground speed output at 451 knots. This speed is much closer to the GPS ground speed than is the ground speed from radar or the PID Estimator. In this flight segment, the hybrid filter significantly outperforms the radar and the PID Estimator.

A similar situation is shown in Figure 24 for a flight segment identified as Turn 7 and 8. This segment has a level segment, followed by a climb, followed by another level segment. Two turns are involved, one of 166 degrees and one of 10 degrees. The GPS ground speed stays relatively constant over the duration of the segment beginning at 445 knots and slowly falling to 425 knots at the end of the segment. The ground speeds from the radar and the PID Estimator both exhibit behavior similar to Figure 23. The radar ground speed falls to 245 knots at 64855 and the output of the PID Estimator is 258 knots at 64890 seconds. The output of the DT&C-R filter is triggered into coast mode at 64762 with a ground speed output of 425 knots. This ground speed closely matches the GPS ground speed for the duration of the coast period. The coast period terminates at 64940 and there is a moderate negative spike to 380 knots. This spike is short-lived as the radar ground speed is “catching up” to the GPS ground speed. In this flight segment, the hybrid filter significantly outperforms the radar and the PID Estimator.

Similar performance is shown in Figure 25 for a very long coast period beginning at 66838. This coast period last for 622 seconds (over 10 minutes). The aircraft is level throughout this segment. There are three measurable turns during this time – 105 degrees, 360 degrees, and 42 degrees. These turns cause huge errors in the radar and PID Estimator values for ground speed – exceeding 200 knots at times. The error for the DT&C-R hybrid filter never exceeds 50 knots and is often less than 20 knots. The average error for the DT&C-R filter during the coast period is –27 knots. The average error for the radar ground speed during this time is –102 knots and the average error for the PID Estimator output is –108 knots.

During Flight 728 there were 17 instances of the DT&C hybrid filter going into coast mode. These coast periods lasted from a minimum of 60 seconds to a maximum of 622 seconds. Table 3 presents a statistical assessment of the performance for the DT&C-R filter compared to GPS. Table 4 presents the same assessment for the DT&C-P filter compared to GPS. The columns related to mean values are shaded for easier identification. Summary statistics for the entire flight are shown at the bottom of the columns. The statistics display the same mixed performance as do the analysis of the graphs.

In general, both the DT&C-R and DT&C-P hybrid filters work significantly better during periods of level flight than during climbing and descending flight. During climbing flight, the output of the hybrid filters was too low. During descending flight the output of the hybrid filters was too high. This observation suggests that it might be prudent to investigate the use of correction factors during these flight phases.

In the cases studied, the DT&C-R filter configuration generally outperformed the DT&C-P filter configuration. This observation is made on a very limited number of PID Estimator assessments, so this observation should not be regarded as conclusive.

Table 3 Statistical Assessment of DT&C-R Hybrid Filter Performance

Coast Segment	Coast Start (sec)	Coast End (sec)	Duration (Seconds)	Radar – GPS		DT&C-R – GPS		Qualitative Rating (Mean)
				Mean (knots)	STDev (knots)	Mean (knots)	STDev (knots)	
1	61592	61694	102	-20.7	11.5	-39.5	17.6	Worse
2	62818	63050	232	-21.3	25.4	-22.6	4.4	Worse
3	63170	63250	80	-12.2	3.5	14.1	1.5	Worse
4	63830	64066	236	-79.2	34.8	24.3	4.6	Better
5	64762	64940	178	-112.0	42.0	-3.4	5.5	Better
6	65634	65734	100	2.6	4.6	55.7	6.5	Worse
7	65856	66048	192	-54.2	26.1	-38.0	6.6	Better
8	66838	67460	622	-101.5	70.7	-27.0	17.6	Better
9	68038	68144	106	-4.8	4.9	53.7	5.1	Worse
10	68268	68412	144	-118.2	57.9	-67.6	6.2	Better
11	68612	68694	82	-1.6	15.9	-24.1	2.4	Worse
12	69092	69238	146	-47.8	20.9	-12.7	7.2	Better
13	69428	69574	146	-50.9	14.7	-13.2	6.8	Better
14	69578	69996	418	-98.9	84.8	-52.1	6.2	Better
15	70030	70090	60	15.7	6.1	-21.1	3.4	Worse
16	70138	70218	80	18.5	4.6	51.8	11.2	Worse
17	70262	70324	62	23.4	11.7	44.1	15.6	Worse
Entire Flight				-23.4	49.9	-7.1	24.4	Better

Table 4 Statistical Assessment of DT&C-P Hybrid Filter Performance

Coast Segment	Coast Start (sec)	Coast End (sec)	Duration (Seconds)	PID – GPS		DT&C-P – GPS		Qualitative Rating (Mean)
				Mean (knots)	STDev (knots)	Mean (knots)	STDev (knots)	
1	61592	61694	102	-50.7	19.8	-40.5	17.6	Better
2	62818	63050	232	-68.4	17.2	-29.2	4.4	Better
3	63170	63250	80	-6.9	13.4	-18.6	1.5	Worse
4	63830	64066	236	-66.2	40.9	23.7	4.6	Better
5	64762	64940	178	-94.3	54.3	-5.7	5.5	Better
6	65634	65734	100	17.2	12.7	58.7	6.5	Worse
7	65856	66048	192	-75.1	19.9	-35.5	6.6	Better
8	66838	67460	622	-107.5	60.7	-28.0	17.6	Better
9	68038	68144	106	13.1	14.9	48.0	5.1	Worse
10	68268	68412	144	-100.6	79.5	-51.3	6.2	Better
11	68612	68694	82	-8.1	6.0	-17.8	2.4	Worse
12	69092	69238	146	-77.0	32.2	-2.6	7.2	Better
13	69428	69574	146	-60.1	18.7	-21.5	6.8	Better
14	69578	69996	418	-101.5	65.0	-92.8	6.2	Better
15	70030	70090	60	-45.4	11.1	-104.4	3.4	Worse
16	70138	70218	80	3.8	11.0	-1.3	11.2	Better
17	70262	70324	62	19.6	10.6	46.9	15.6	Worse
Entire Flight				-29.0	50.0	-13.5	31.6	Better

Analysis – Post-Flight Determination of Track Adherence

This section of the report investigates the use of processed radar data to determine track adherence of aircraft operating in the NAS. The FAA's Host Computer System provides information regarding aircraft intent in the form of flight plans, and aircraft state, which is derived from measurements derived from the FAA's radar tracking system. The state information is in the form of:

- position – horizontal X, Y position of the aircraft measured in local stereographic projection coordinates (units are in Nautical Miles (NM))
- altitude – Mode C altitude of the aircraft in 100's of feet
- ground speed – ground speed of the aircraft (knots)
- vertical speed – vertical speed of the aircraft (feet/minute)
- time – time (measured in seconds) of the data record (measured in Universal Coordinated Time (UTC))

Track adherence is basically a comparison of radar track information to flight plan information with computations and logic to determine if aircraft are within some predetermined threshold distance from their flight plan route. Track adherence is a two-dimensional problem restricted to the horizontal plane.

Track Adherence in Straight Flight Segments

Track adherence during the straight segments of the flight plan is straightforward. Diagram 2 represents an aircraft at location X_A, Y_A whose intended track has X_N, Y_N as an origin point and X_{N+1}, Y_{N+1} as a destination point. The distance D_{CT} represents the cross track error, which is the measure of track adherence. The cross track distance can be easily calculated from vector relationships using the information on the diagram.

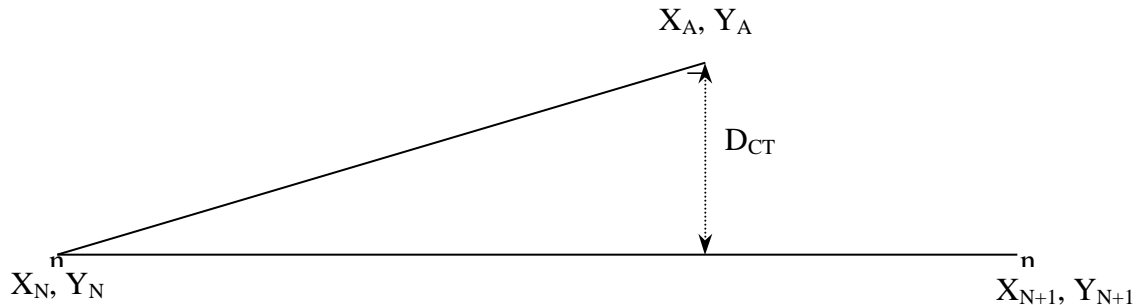


Diagram 2 Track Adherence during Straight Segments of a Flight

Track Adherence at Turn Points

When there is a turn in the flight plan, the process of determining the adherence to the flight plan becomes more complex. Diagram 3 represents two straight segments of a flight plan with a turn of approximately 45 degrees at the point where the two segments meet. Because the aircraft can not turn instantaneously, the aircraft's course will typically follow some curved path around the turn. Aircraft using flight management systems have positive course guidance and typically fly a circular arc with some radius R around the turn as shown in Diagram 3. Other aircraft with less sophisticated guidance systems may follow courses that overshoot or undershoot the turn as indicated on the diagram. The circular path shown in the diagram best represents the

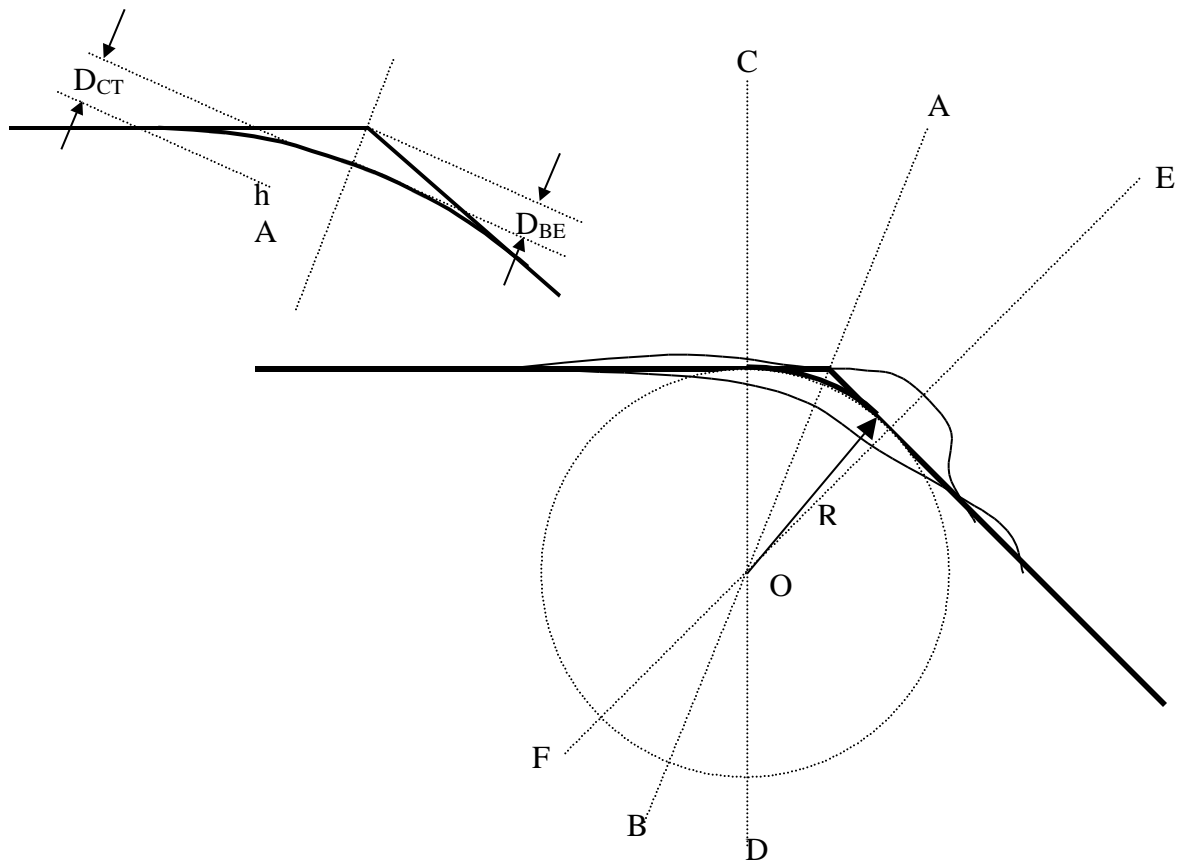


Diagram 3 Cross Track Error Determination During a Turn

measurement of cross track error at turn points. The magnitude of the radius R is a function of the speed and turn rate of the aircraft. For a typical transport jet aircraft, assuming a speed of 450 knots and a turn rate of 60 degrees per minute at cruise altitude, the turn radius would be on the order of 7 NM.

Track Adherence – Angle Bisector Methodology

One possible means of determining the cross track error during the turn is to use the angle bisector (line AB) as the boundary between the first and second segments of the flight plan. When the aircraft is in each segment, the technique described in the previous paragraph can be used to determine the cross track error and track adherence. The bisector methodology has an inherent problem in representing the cross track error at the turn point. A false cross track error will be generated when the aircraft is in the turn. An aircraft following a circular arc course around the curved segment at the turn point will experience this false bisector error (represented by D_{BE} in the inset) while in the region bounded by lines CD and EF . This error will reach a peak at the bisector. The magnitude of the error will depend on the magnitude of the turn and the turn radius R . Examples of this error are shown in Table 5 for a turn radius of 7 NM. For turns of small magnitudes, the method works reasonably well, but the error introduced by the bisector methodology begins to grow rapidly as the turn magnitude increases. If the method was used when an aircraft goes into a holding pattern, which has an initial turn of 180 degrees, or if the aircraft performs a 360 degree turn, the definition of the bisector becomes unusable and the methodology breaks down.

Table 5 Inherent Cross Track Error at Turn Points Caused by Use of the Angle Bisector Methodology (Turn Radius = 7 NM)

Turn Magnitude (Degrees)	D_{BE} – Inherent Bisector Error Caused by Bisector Methodology (NM)
15	0.06
30	0.25
45	0.58
90	2.90
135	11.29

Track Adherence – Curved Segment Methodology

A second method of measuring the cross track error during the turn is to add a turn segment to the definition of the flight path. The flight path shown in Diagram 3 would consist of a straight segment to line CD, a curved segment from line CD to line EF, and a straight segment beyond line EF. Cross track error in the curved segment (represented by D_{CT} for an aircraft located at point A in the inset in Diagram 3) is measured with respect to the circular arc with radius R. This methodology produces a cross track error that closely models the “perfect track” described previously. The major disadvantage to this technique is that cross track error is not defined for aircraft that fly through the region bounded by points FOD, which represents an extreme undershoot situation. This situation is not likely if the radius R is made large enough to minimize these occurrences. In operational situations, aircraft tend to overshoot rather than undershoot turns. Therefore, this problem is not considered a serious drawback to the curved segment methodology.

Application of the curved segment methodology requires that turn segments be identifiable in both the flight plan and radar track information. The process of identifying turns in the flight plan information is quite straightforward when solved by applying vector techniques to the flight plan data. However, identifying corresponding turns from radar data is more problematic. The noise in position, ground speed and track information inherent in the radar data causes errors in detecting these turns. The filtering methods described in prior sections of the report can be applied to improve the turn detection process. Since the track adherence determination is performed in a post-flight environment, opportunities exist to use correction procedures on the processed data to reduce the delay effects encountered in the data processing filters.

Track Angle Identification and Delay Correction

In analyses described earlier in the report, the PID Estimator shown in Diagram 1 was found to be an effective means of determining the track angle of the aircraft. The major problem with the track angle output of the filter was the delay inherent in the filter process. Figures 9 and 10 showed graphical evidence that the track angle output of the PID Estimator (with a time constant of 20 seconds) closely followed the GPS track angle. The delay introduced by the PID Estimator was quantified by performing a correlation between the GPS track angle data and a time-shifted

track angle output of the PID Estimator. The amount of time shift was varied from 0 to 100 seconds. The output of the correlation process is shown in Figure 26. The point where the correlation function reaches a peak (correlation value of .9916 at 54 seconds) corresponds to the appropriate delay value to be used in the correction process. It should be noted that different time constants and different filter configurations produce different correlation results. The time-shift correlation process should be performed again if other filter configurations are used.

Because the PID Estimator has fixed gain constants, delay values are stable and do not vary as a function of the input data characteristics. This is not necessarily true with other estimator concepts. For example, gains in the Kalman Filter Estimator are time varying according to the covariance error measured during the filtering process. This characteristic of filters with adaptable gains makes them less suitable for delay correction during post-flight data analysis.

The track angle output of the PID Estimator (time-shifted by 54 seconds) is compared with the GPS track angle data in Figures 27 and 28. With the exception of the points in the vicinity of 68285 seconds (highlighted by the magenta ellipse), the difference between these two curves is barely perceptible in these figures.

The problem at 68285 seconds can be easily explained by looking at the unusual character of the X, Y data in Figure 6. The track angle abruptly shifts from 90 degrees to 235 degrees to 50 degrees to 130 degrees to 45 degrees all in the space of a few data points. As discussed earlier in the report, this is likely caused by idiosyncrasies in the radar system and it does not represent the true flight path characteristics of the aircraft in this region.

The error in the time-shifted PID Estimator output of track angle was calculated by subtracting the GPS track angle. The graph of the result is shown in Figures 29 and 30. The error shows some high frequency content which is hardly evident when looking at the track angle output of the PID Estimator in Figures 27 and 28. The mean and standard deviation of the error in track angle were calculated from the time series shown in Figures 29 and 30. The area around 68285 seconds is highlighted by the magenta ellipse in the figures. Two sets of error statistics were calculated. One set included the errors in the vicinity of 68285 seconds and the second set eliminated errors greater than 5 degrees in this area, treating these errors as outliers. The results of the statistical calculations are shown in Table 6.

Table 6 Error in Time-Shifted Track Angle Output of PID Estimator (TC = 20 seconds)

Metric	All Points Included (degrees)	Outliers Removed (degrees)
Mean	-0.2	-0.6
Standard Deviation	6.3	3.0
Maximum Error	100.0	11.7
Minimum Error	-15.1	-15.1

As one final test of the time-shifted track angle output of the PID Estimator, the turn rate was calculated from the output and subjected to the criteria for turning flight (turn rate > 30 degrees/minute) used earlier in the analyses. The results are graphically compared with the GPS results in Figures 31 through 33. The PID turn indicator matches the GPS turn indicator

throughout most of the flight with some exceptions. The PID indicator does not identify the 10-degree turn just before 65000 seconds as shown in Figure 32. The PID indicator identifies some small turns just prior to 67000 seconds, but the GPS turn indicator does not identify these turns. The PID turn indicator does not identify a 30-degree turn just after 69500 seconds but does identify a small turn about 60 seconds after the GPS identifies the 30-degree turn. The PID turn indicator also identifies two small turns after 70000 seconds that are not identified by the GPS turn indicator.

The correlation between the GPS turn indicator and the PID turn indicator was calculated to be 0.8528. A value of 1.00 would indicate total agreement between the two indicators. The track angles had a high degree of correlation that was greater than 0.99. Because the turn indicators are based on the time derivative of the track data, noise in the PID output data causes the turn indicator data to have a lesser degree of correlation than the track angle data.

The turn rate threshold for these calculations was set at 30 degrees/minutes. Modifications to the turn indicator logic (such as selecting higher or lower thresholds for turn detection) will affect the missed-turn rate and the false-turn rate. This threshold can be modified depending on the application and its sensitivity to missed-turns or false-turns.

Conclusions and Recommendations

Conclusions - Application of the Hybrid Filter Concept to Velocity Estimation for DSTs

The hybrid filter concepts investigated in this study require additional conceptual development, analysis and testing before they can be considered for use in CTAS or other DST's. The major findings in this limited investigation are as follows:

1. The PID Estimator with inputs from the FAA's Host Computer System is useful in identifying turns in the aircraft's ground track. Turning segments of the aircraft track were reliably identified and the magnitudes of the turns were accurately determined. The main concern with the turn point identification is delay caused by the need to filter the source data. The best performing filter in this assessment exhibited a 54-second delay in identifying start and end points of the turn. This delay may adversely impact DSTs that require real-time turn point identification. The delay can be compensated in a post-processing environment by applying time-shift techniques to the PID Estimator output data for the aircraft track and turn points.
2. The hybrid filters improved ground speed estimation during large magnitude turns in level flight. These improvements were quite dramatic in many instances reducing ground speed errors in excess of 200 knots to 50 knots or less. However, operational occurrences of large magnitude turns are not often encountered in the NAS except during holding operations and 360-degree turns for spacing. These are precisely the operations that DST's are intended to eliminate or at least minimize. Therefore, the application to large magnitude level turns is not considered to be useful for broad application in the NAS.
3. For small magnitude turns the performance of the hybrid filters was generally worse than using either radar ground speed estimates or PID Estimator outputs for ground speed. For five turns ranging from 22 to 52 degrees, the performance of the DT&C-R filter was worse than the radar ground speed and the performance of the DT&C-P filter was better than the PID ground speed in 2 cases and worse in 3 cases.
4. During turns while the aircraft is climbing, the ground speed output of the hybrid filters is less than the actual ground speed of the aircraft by 50 knots or more. During turns while the aircraft is descending, the ground speed output of the hybrid filters is greater than the actual ground speed of the aircraft by 50 knots or more. Both situations are caused by delays in identifying turn points caused by the need to filter aircraft track data. These results suggest that ground speed compensation during climbs and descents might improve performance of the hybrid filters. Additional analysis is needed to confirm the benefits of such compensation.
5. Because the source data for this analysis was obtained under flight demonstration conditions, it is not representative of trajectories typically found in NAS operations. For this reason, further hybrid filter development work should be tested using flight data that represents a broad range of NAS operations.

Conclusions - Application of the Hybrid Filter Concept for Post-Flight Track Adherence Determination

1. The most useful metric for track adherence is cross track error relative to the aircraft flight plan. The cross track error calculation is straightforward for straight segments, but becomes more complex at route turn points.

2. A high fidelity method of measuring track adherence during a turn is to model the turn as a circular arc with radius representative of the aircraft speed and turn rate. This method will successfully model most turn situations found in the NAS. The geometric construction of this model does become indeterminate if the aircraft severely undershoots the turn by an amount greater than the assumed radius of the turn, but such occurrences are not typical in the NAS.
3. A lesser fidelity method of measuring track adherence during a turn is to separate two straight segments at the angle bisector of the turn. This method has an inherent error that is a maximum at the turn point on the angle bisector. For small turns, this error is quite small and will not significantly affect track adherence determination. However, for turns in excess of 90 degrees, the error becomes significant and may impact track adherence calculations. For turns of 180 degrees the bisector becomes indeterminate and other methods must be employed.
4. Delays in outputs from the PID Estimator, which has fixed gains, can be successfully compensated in a post-processing analysis environment. The method of correlating GPS “truth data” and time-shifted outputs from the PID Estimator yielded track angles that closely tracked the GPS data. This correlation process must be performed each time that filter gain constants are changed in order for the results to be valid.
5. The methodology applied herein for correcting for filter delays may not be valid when applied to Kalman Filter techniques and other filters that have time varying gain constants. When these methods of setting gains are employed, the time shift observed in the output data may change over the duration of the flight depending on characteristics of the input data.
6. Track angle and turn identification methods derived from filtering of radar data, as described in this report, can be useful in the track adherence determination process. Turn magnitudes and turn indicators calculated from the PID Estimator closely matched actual aircraft turn magnitudes and turn indications as measured from GPS data for Flight 728 of the NASA TSRV aircraft. However, the data collected by NASA during the en route descent demonstrations was collected for research purposes. As such, the results of this analysis are not truly representative of actual NAS operations.

Recommendations

1. The linear and hybrid filtering methods for ground speed correction, track angle estimation, and turn indication identified herein require additional research and development before their application to DST's and track adherence can be fully assessed. In particular, the data sets used to perform preliminary assessments of the filtering methods were performed for research purposes and are not typical of NAS operations. The filter characteristics, such as gains and threshold detection levels, should be reassessed using data from actual NAS operations or research flights that model actual NAS operations during significant portions of the flights.

References

1. Chatterji, G. B., "Short-Term Trajectory Prediction Methods," AIAA-99-4233, AIAA Conference on Guidance, Navigation, and Control, Portland, OR, Aug. 1999
2. D'Azzo, J. J. and Houpis, C. H.; Feedback Control System Analysis and Synthesis, McGraw-Hill Book Company, New York, NY, 1960.

Acronyms

ARTCC	Air Route Traffic Control Center
ATAN	Arctangent Function
ATC	Air Traffic Control
ATM	Air Traffic Management
CTAS	Center - TRACON Automation System
DST	Decision Support Tool
DT&C	Detect Turn and Coast Hybrid Ground Speed Filter
DT&C-P	Detect Turn and Coast Hybrid Ground Speed Filter Using PID Estimator Inputs
DT&C-R	Detect Turn and Coast Hybrid Ground Speed Filter Using Radar Inputs
EDA	En Route Descent Advisor
FAA	Federal Aviation Administration
GPS	Global Positioning System
MSL	Mean Sea Level
NAS	National Airspace System
NASA	National Aeronautics and Space Administration
NM	Nautical Miles
PID	Proportional - Integral – Derivative Estimator
SQRT	Square Root Function
TC	Time Constant
TRACON	Terminal Radar Control Area
TSRV	Transport System Research Vehicle
URET	User Request Evaluation Tool
UTC	Universal Coordinated Time
WJHTC	William J. Hughes Technical Center

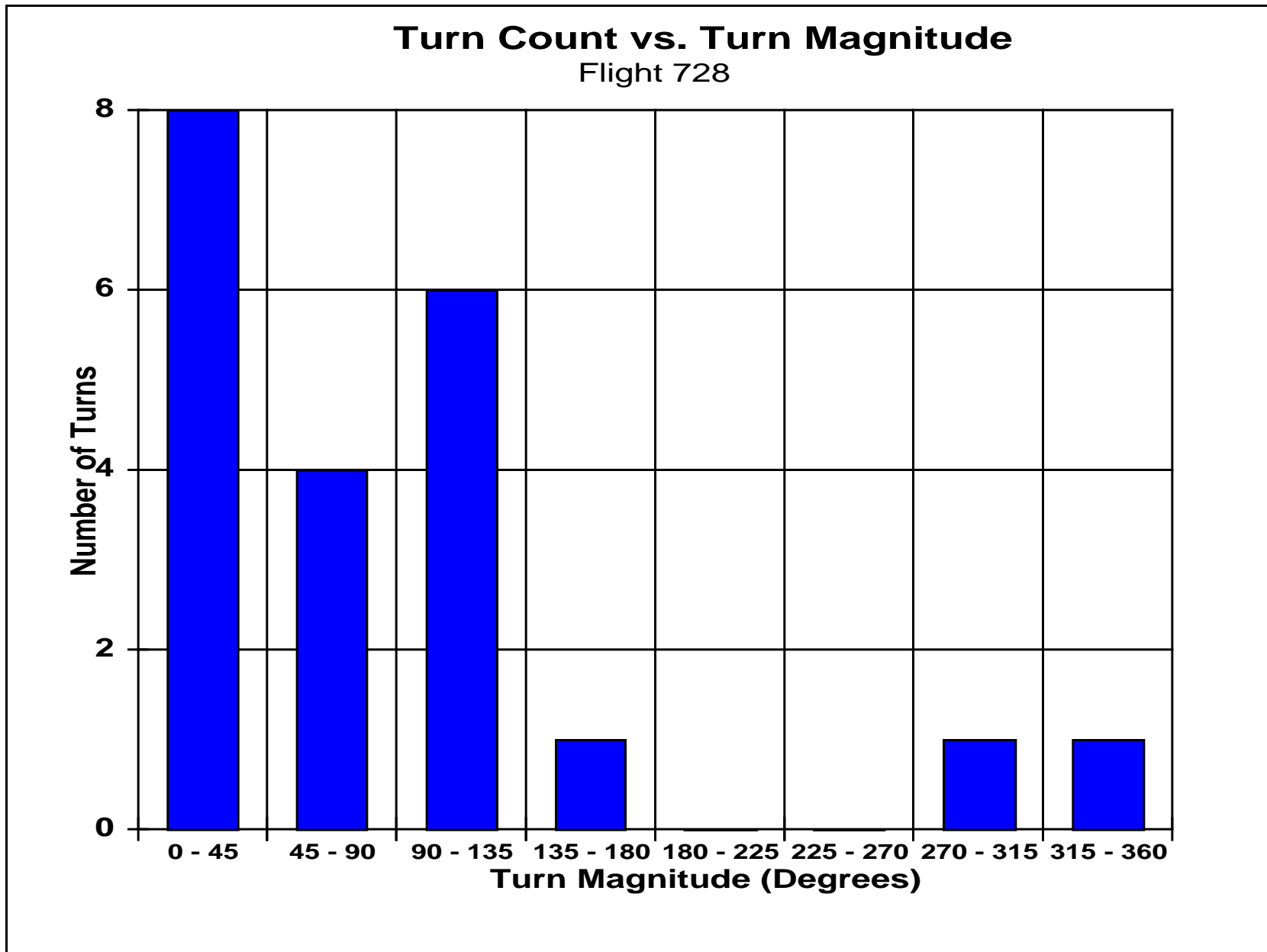


Figure 1 Number and Distribution of Turns for Flight 728

Flight 728

Radar Data

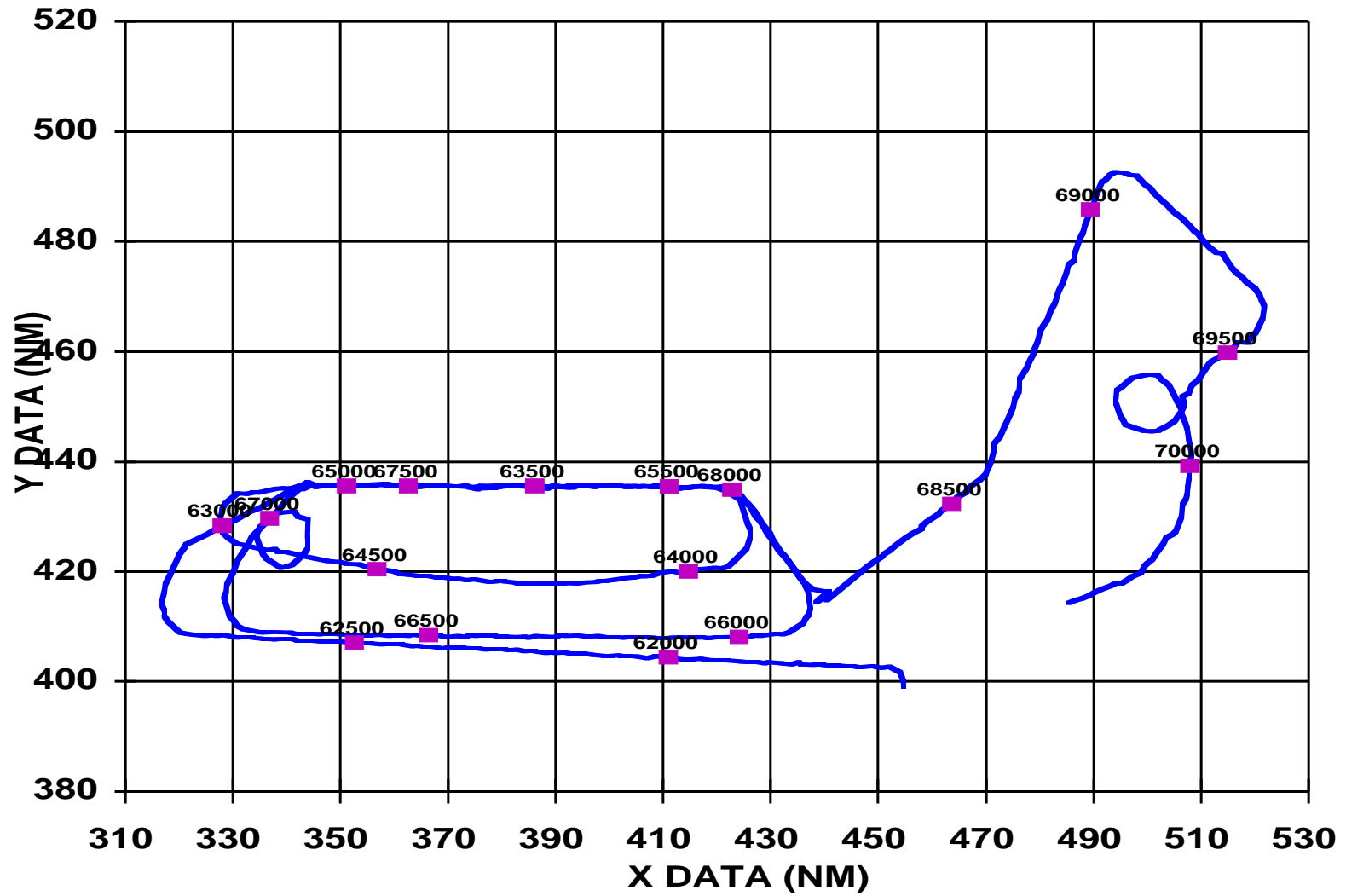


Figure 2 Radar Flight Track of Flight 728

Flight 728

GPS Data

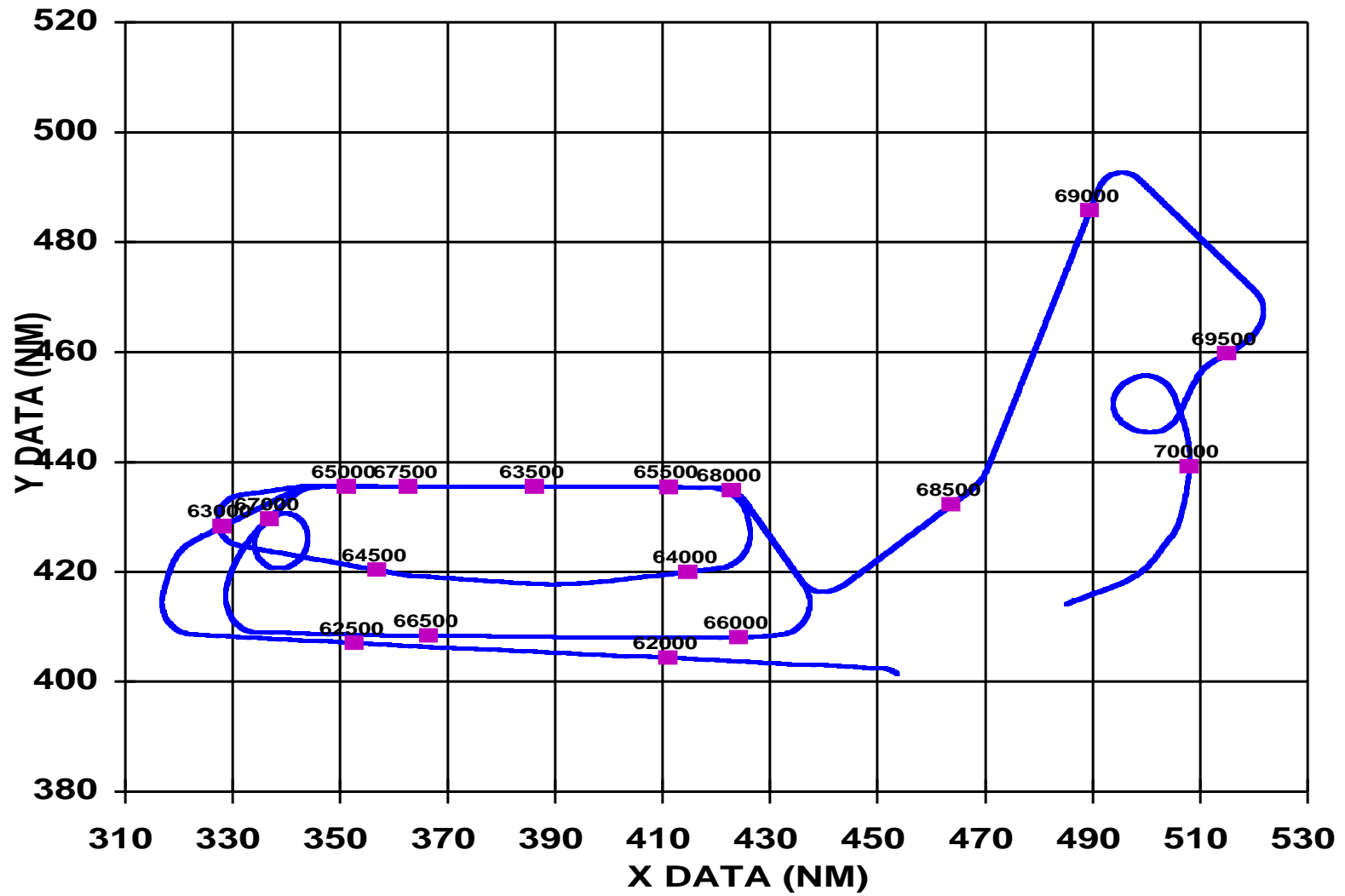


Figure 3 GPS Flight Track of Flight 728

Flight 728 - Small Segment Radar Data

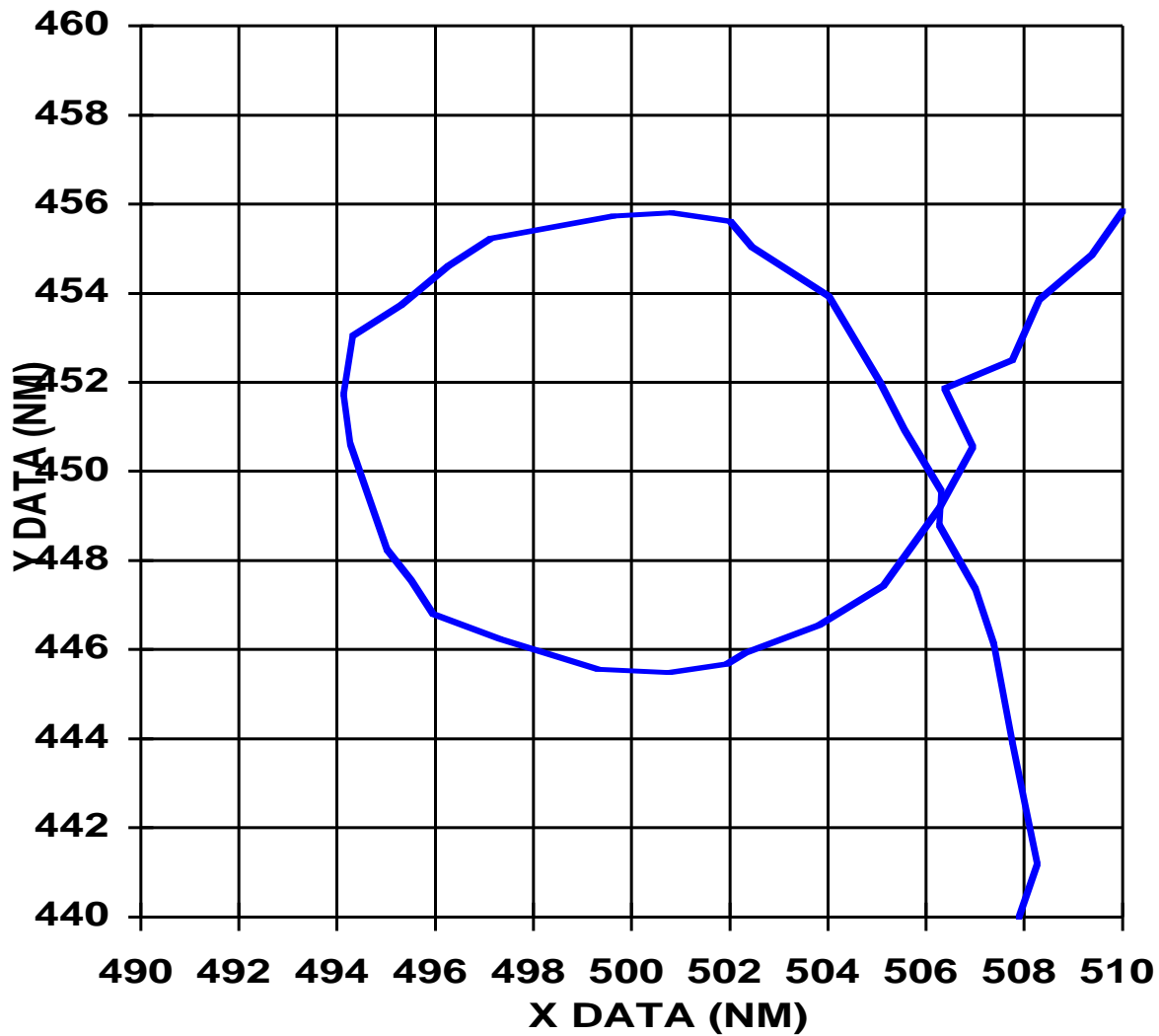


Figure 4 Radar Flight Track for Small Segment of Flight 728

Flight 728 GPS Data

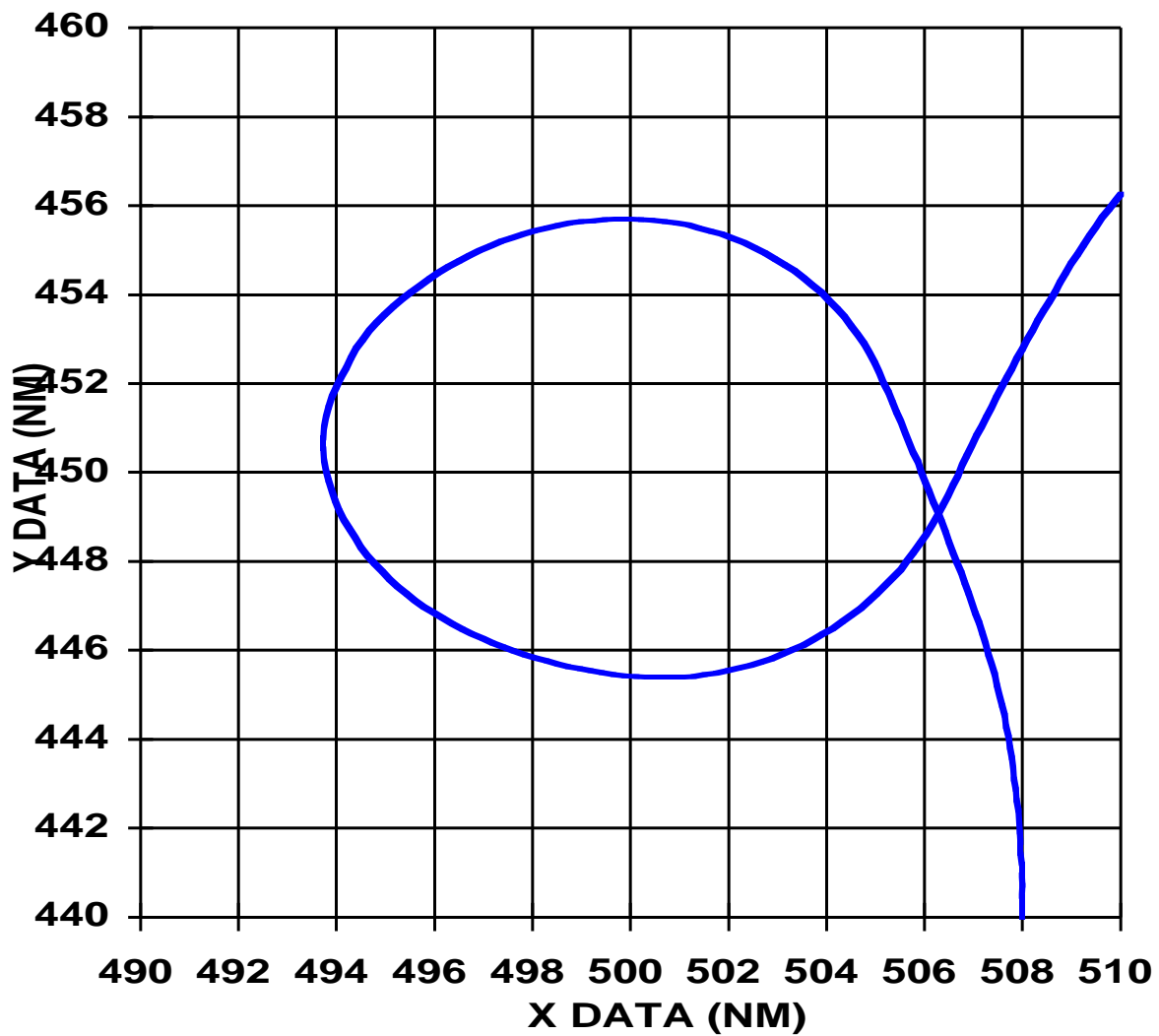


Figure 5 GPS Flight Track for Small Segment of Flight 728

Flight 728 - Unusual Radar Data Points

Radar Data

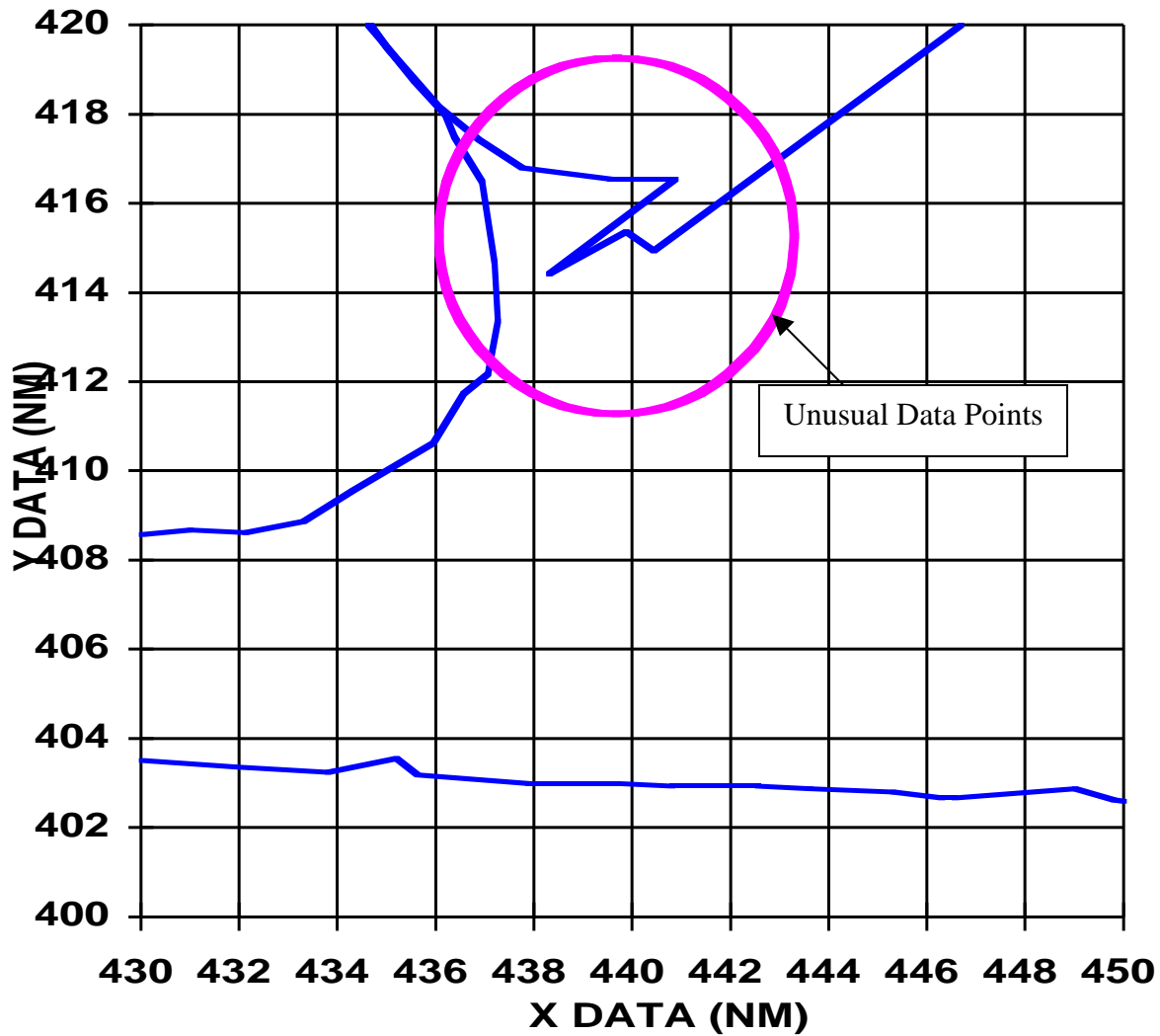


Figure 6 Unusual Data Points for Flight 728 Occurring at Time = 68285 Seconds

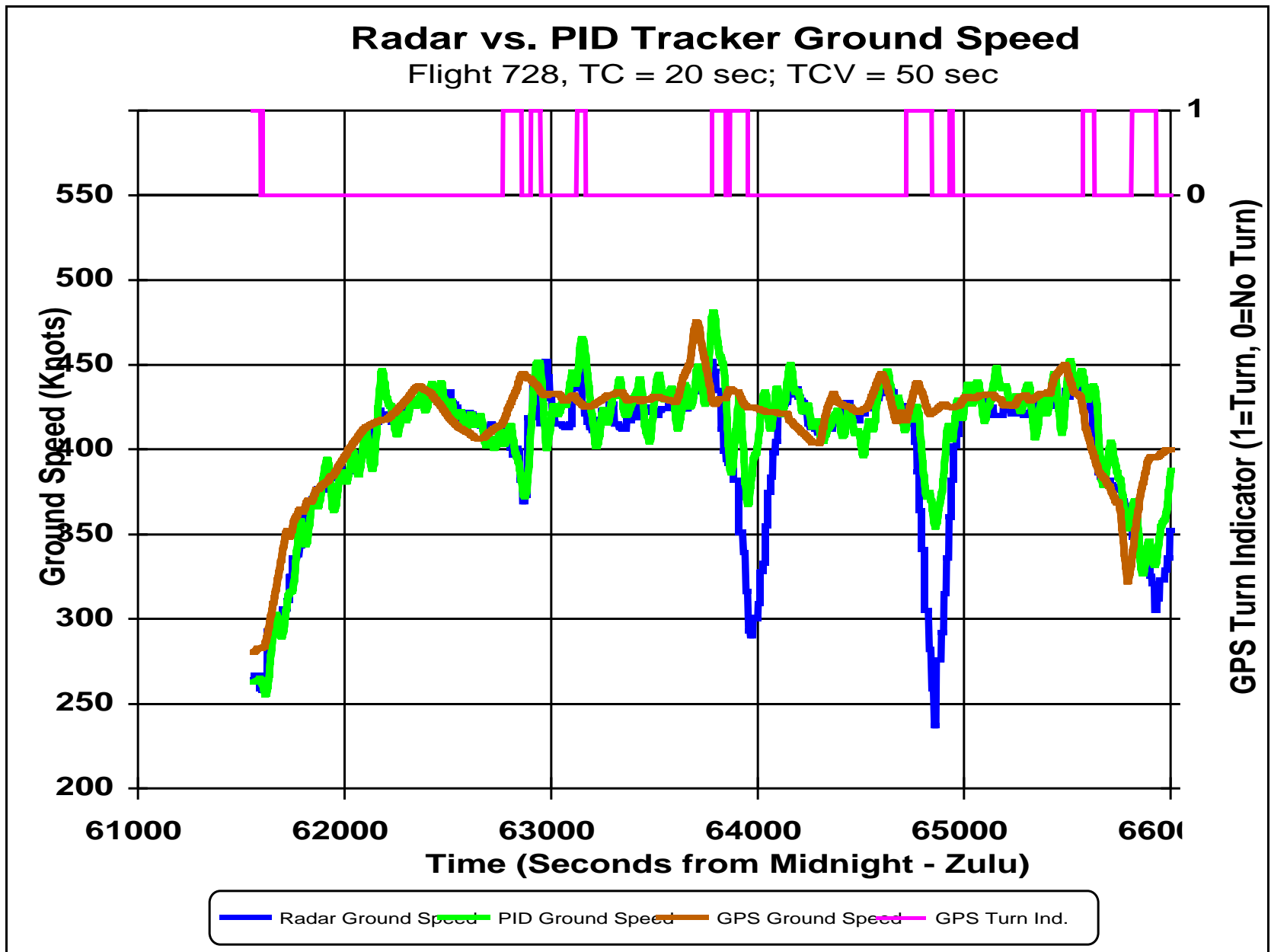


Figure 7 Comparison of Ground Speed for Radar and PID Tracker for First Half of Flight 728 (TC = 20 seconds, TCV = 50 seconds)

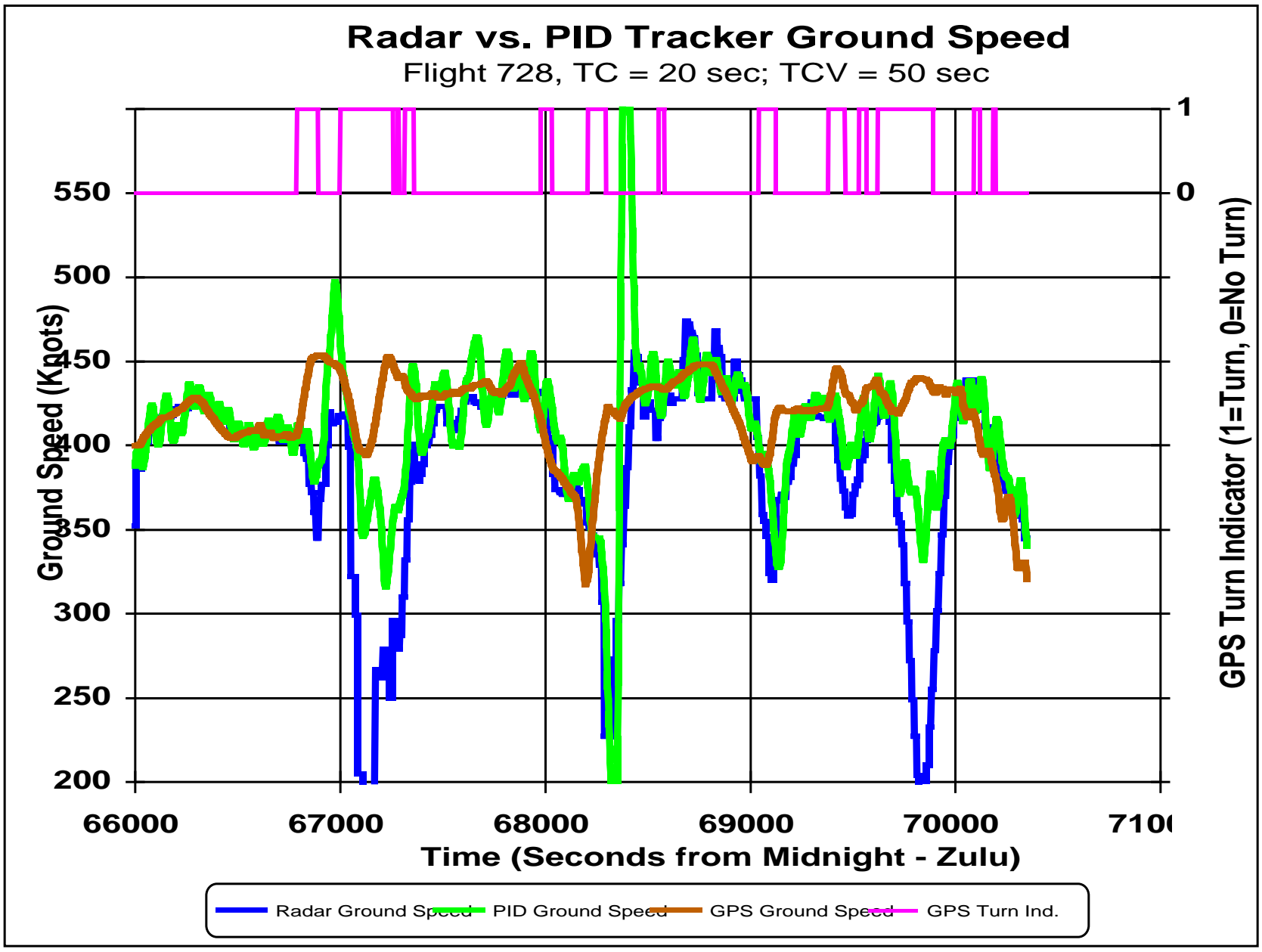


Figure 8 Comparison of Ground Speed for Radar and PID Tracker for Second Half of Flight 728 (TC = 20 seconds, TCV = 50 seconds)

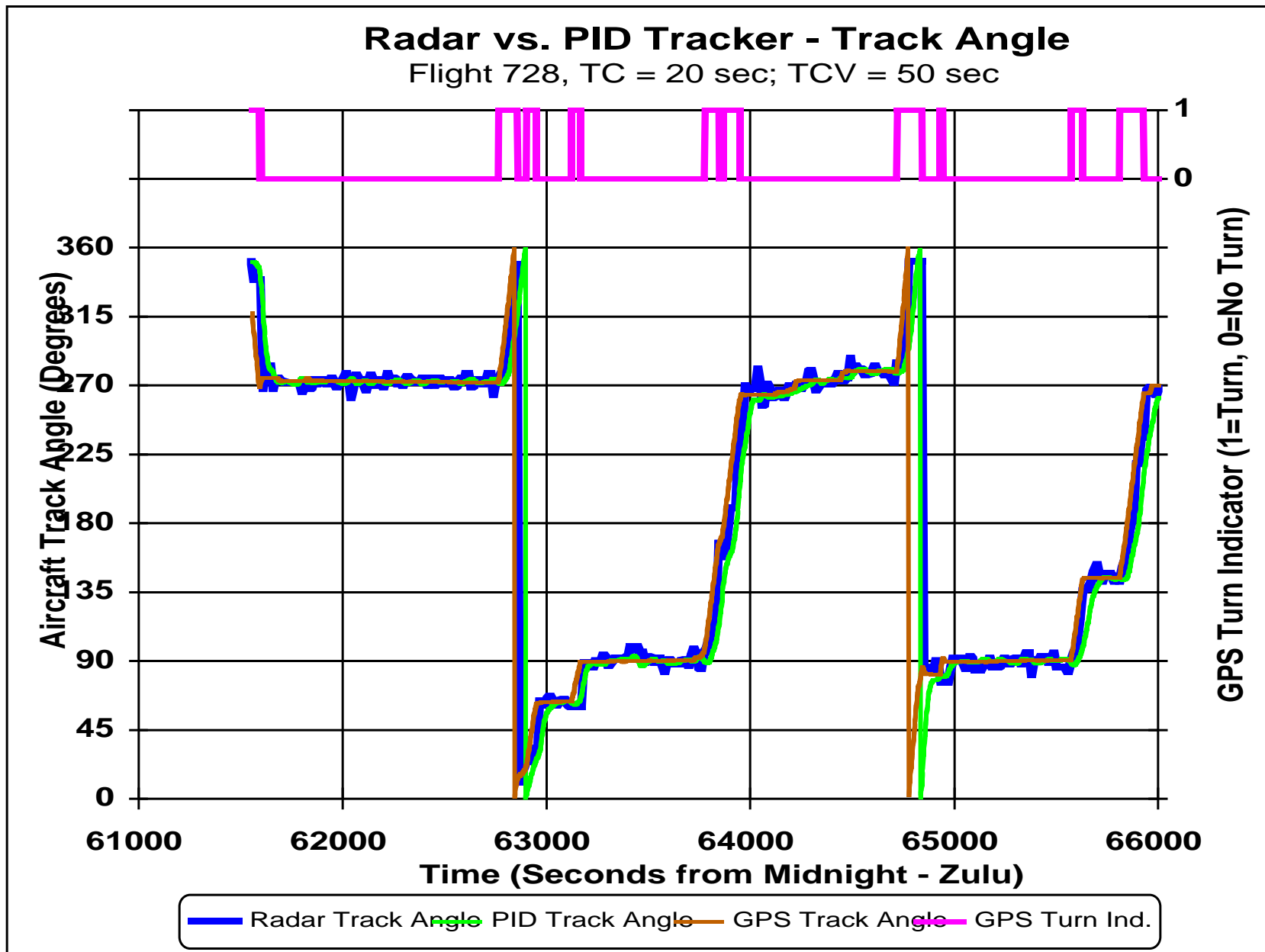


Figure 9 Comparison of Track Angle for Radar and PID Tracker for First Half of Flight 728 (TC = 20 seconds, TCV = 50 seconds)

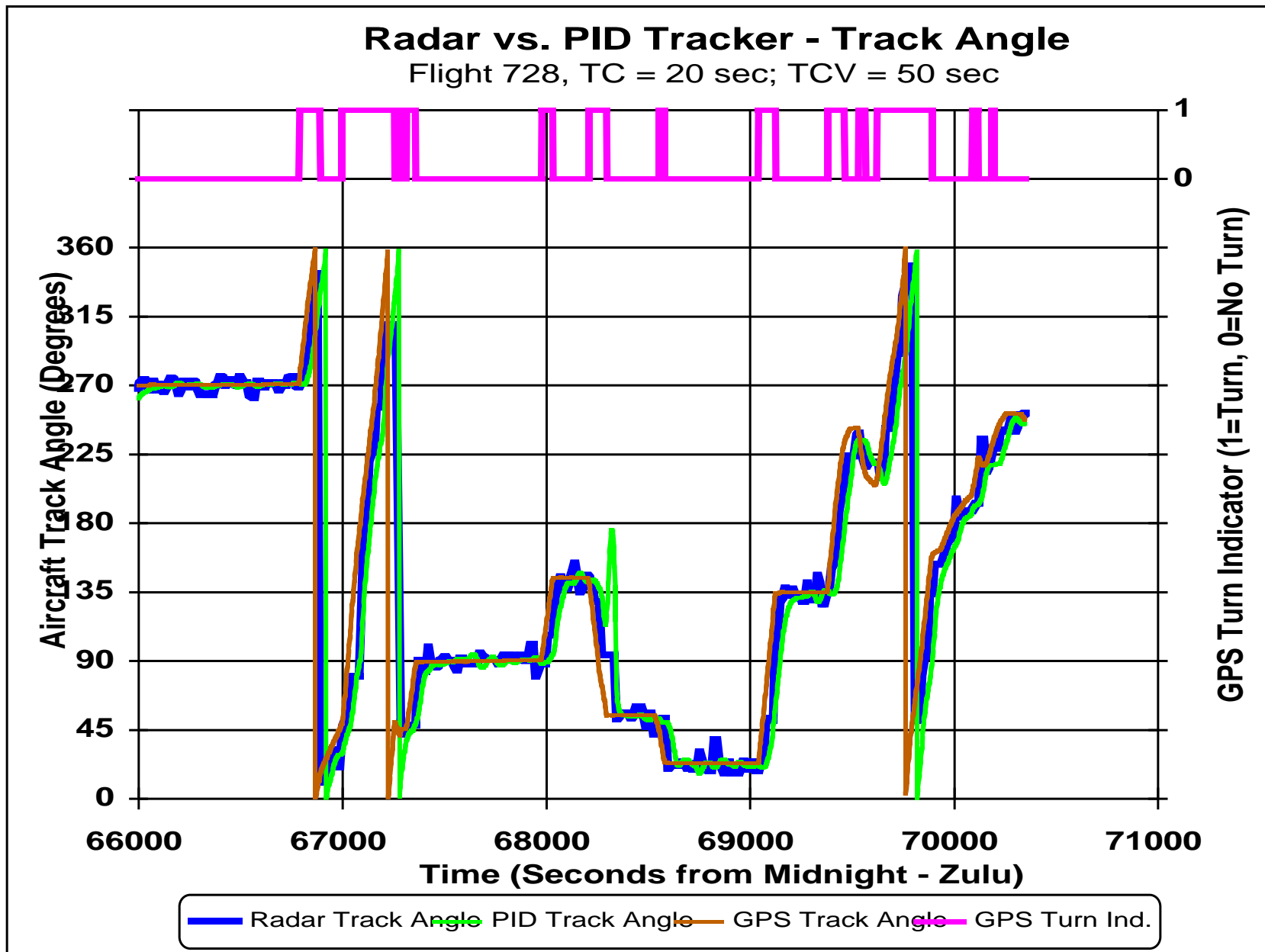


Figure 10 Comparison of Track Angle for Radar and PID Tracker for Second Half of Flight 728 (TC = 20 seconds, TCV = 50 seconds)

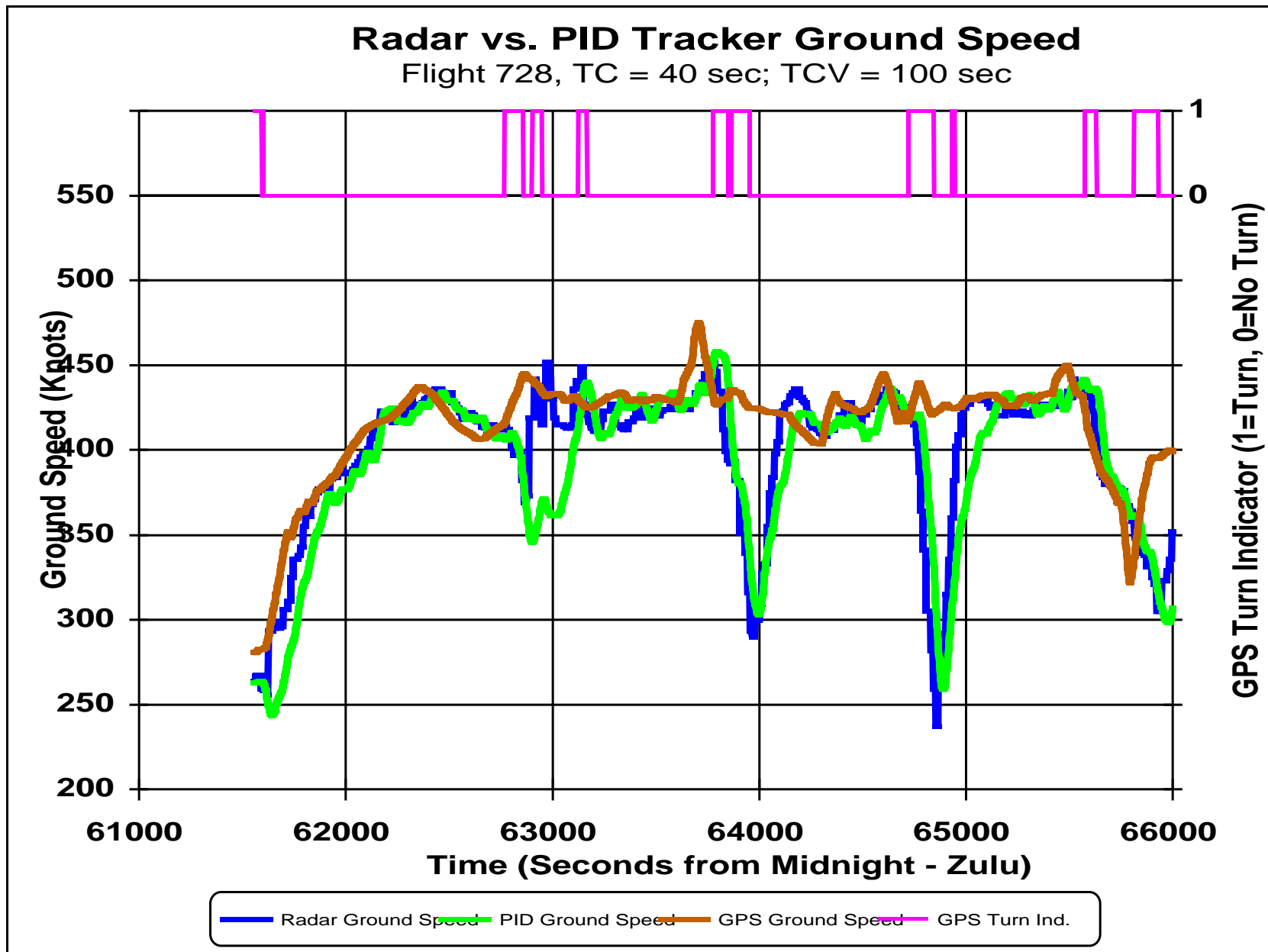


Figure 11 Comparison of Ground Speed for Radar and PID Tracker for First Half of Flight 728 (TC = 40 seconds, TCV = 100 seconds)

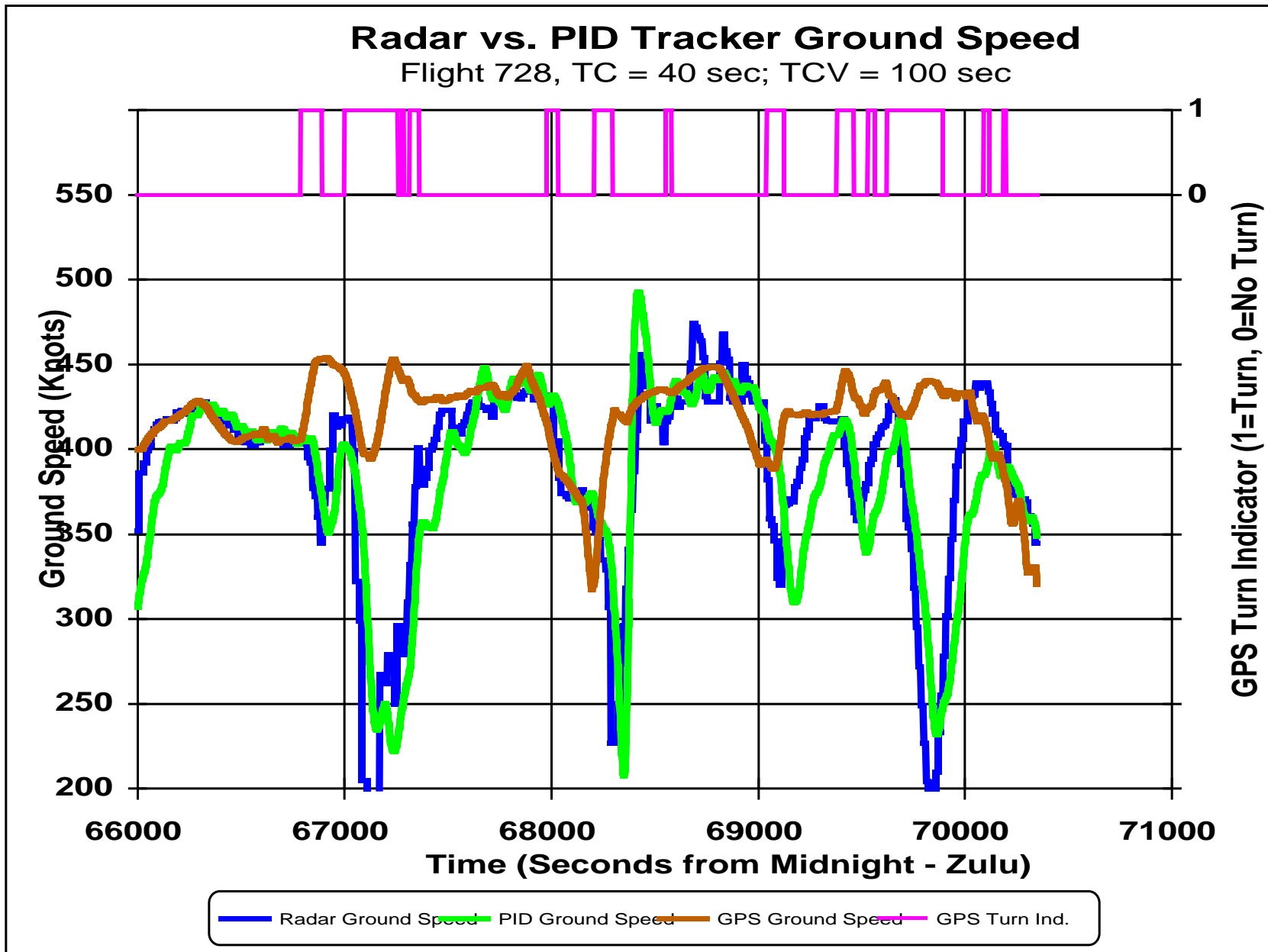


Figure 12 Comparison of Ground Speed for Radar and Hybrid Tracker for Second Half of Flight 728 (TC = 40 seconds, TCV = 100 seconds)

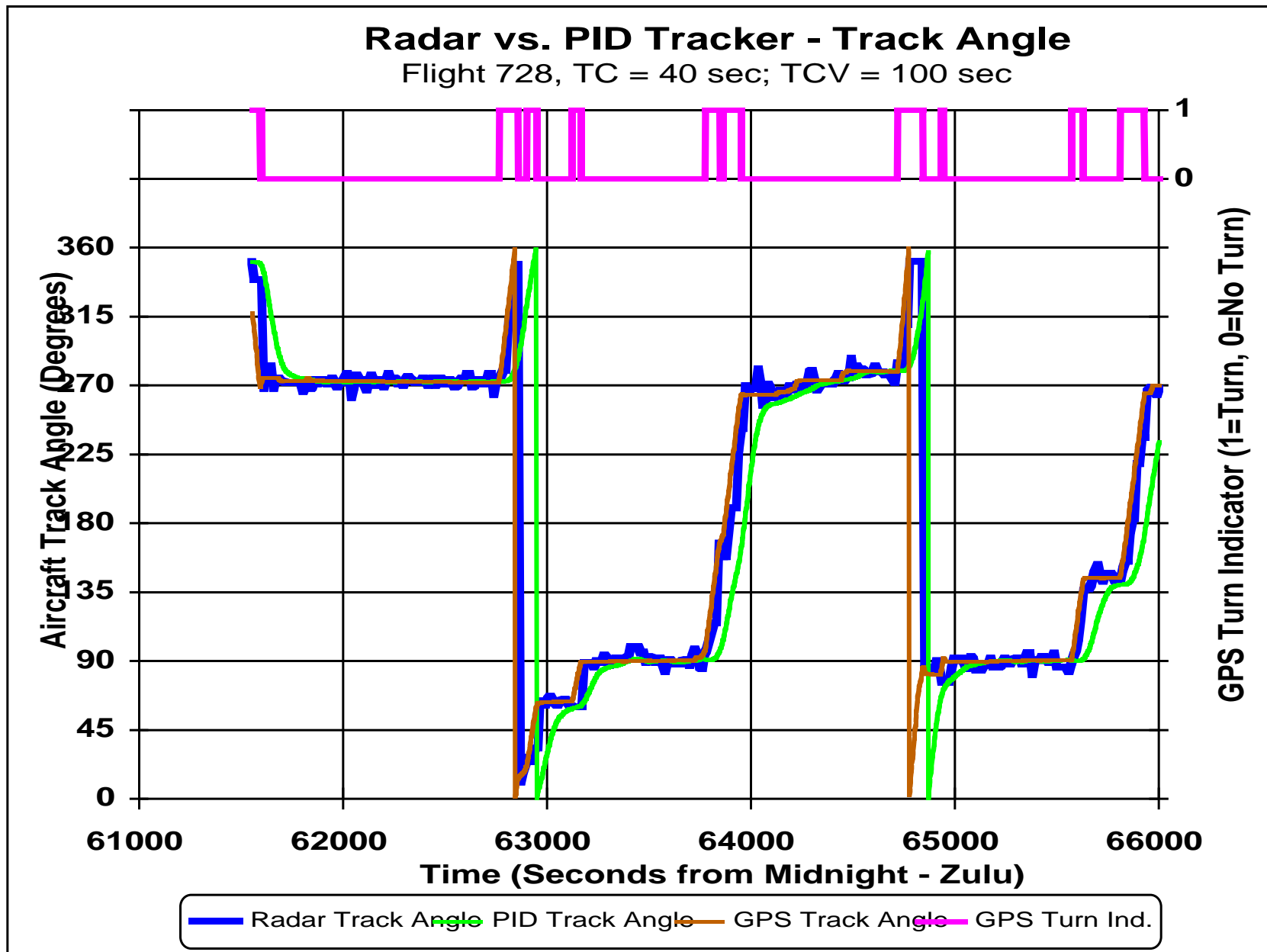


Figure 13 Comparison of Track Angle for Radar and Hybrid Tracker for First Half of Flight 728 (TC = 40 seconds, TCV = 100 seconds)

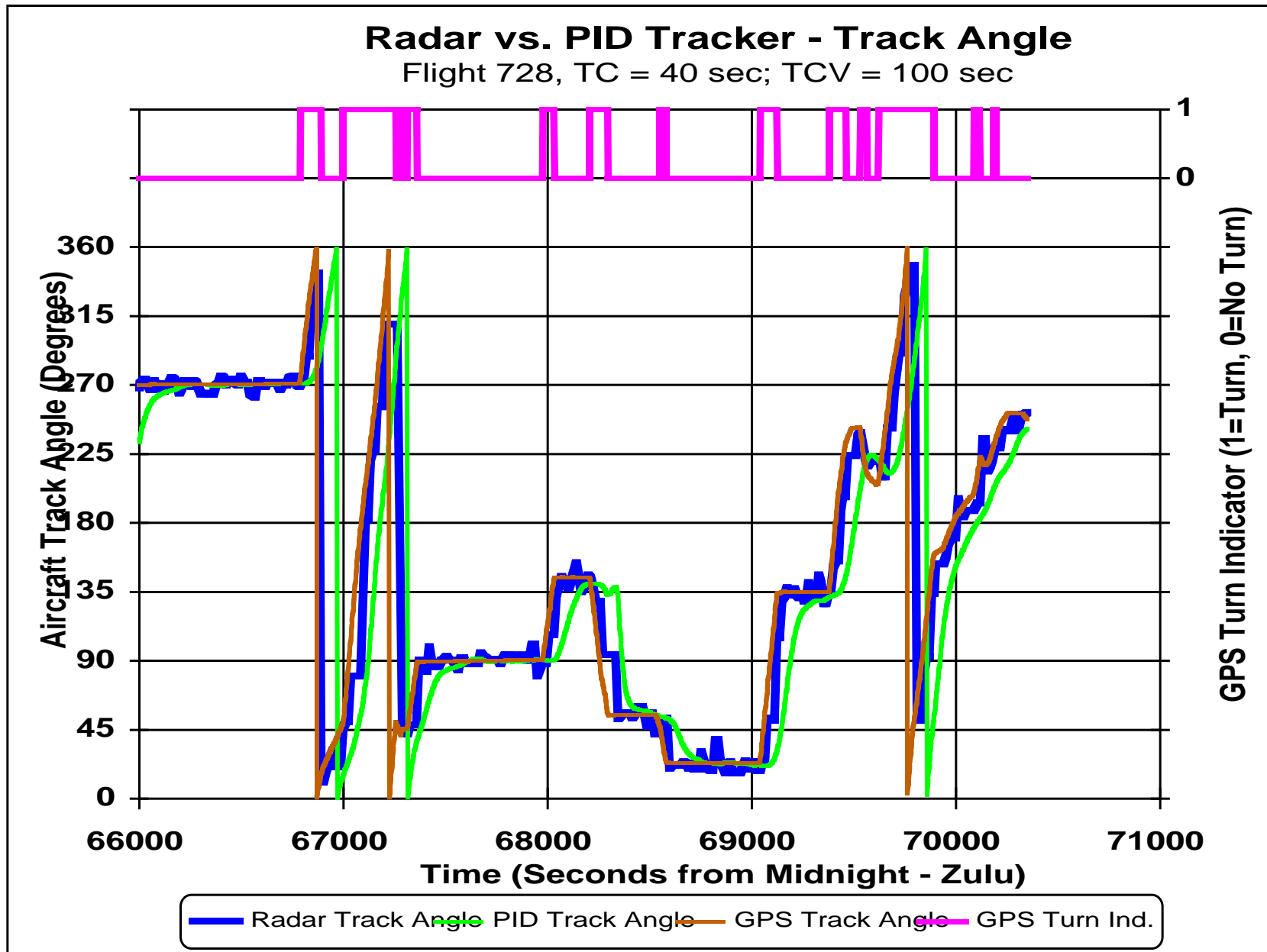


Figure 14 Comparison of Track Angle for Radar and Hybrid Tracker for Second Half of Flight 728 (TC = 40 seconds, TCV = 100 seconds)

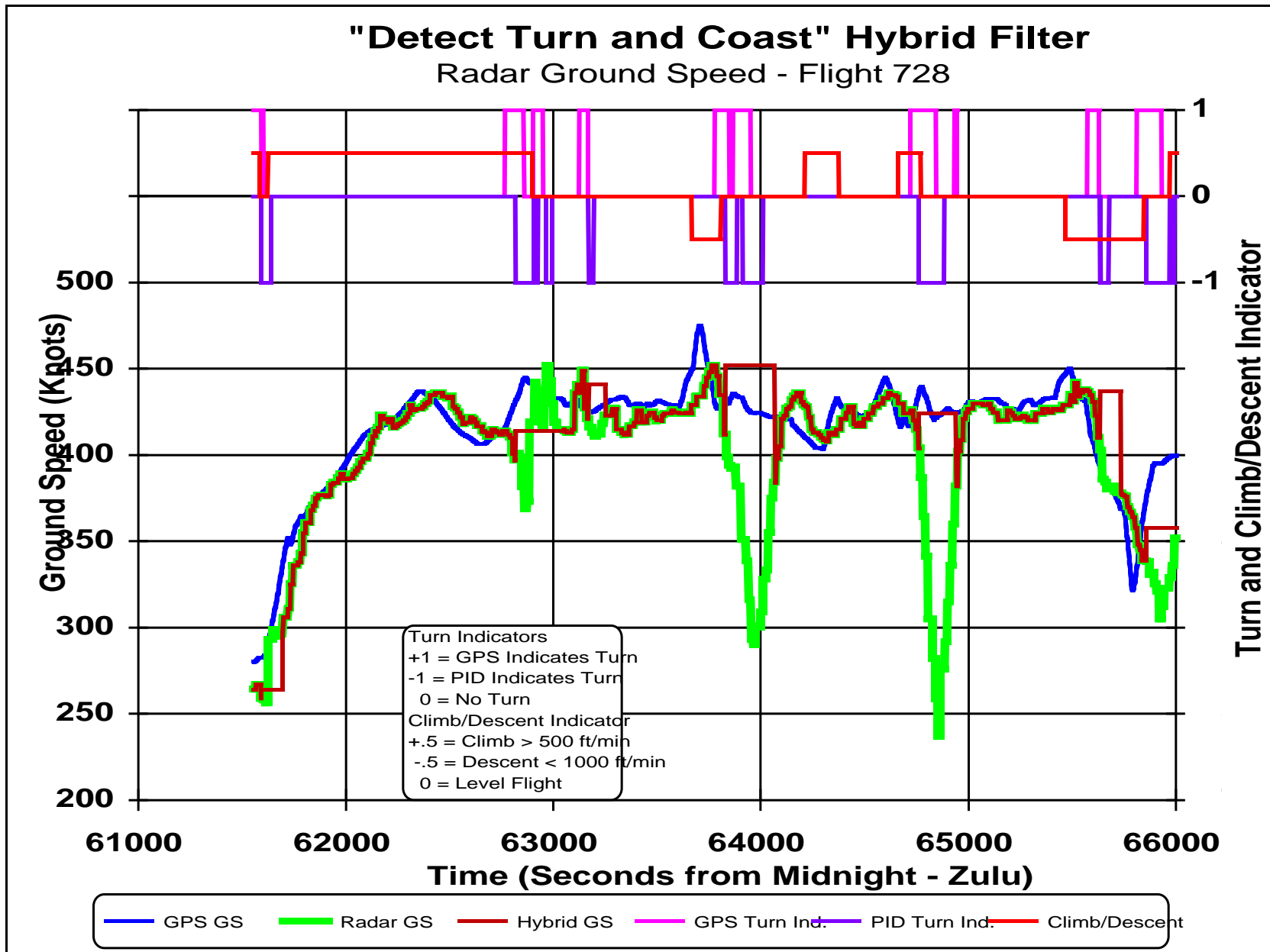


Figure 15 "Detect Turn and Coast" Hybrid Filter Using Radar Ground Speed for First Half of Flight 728

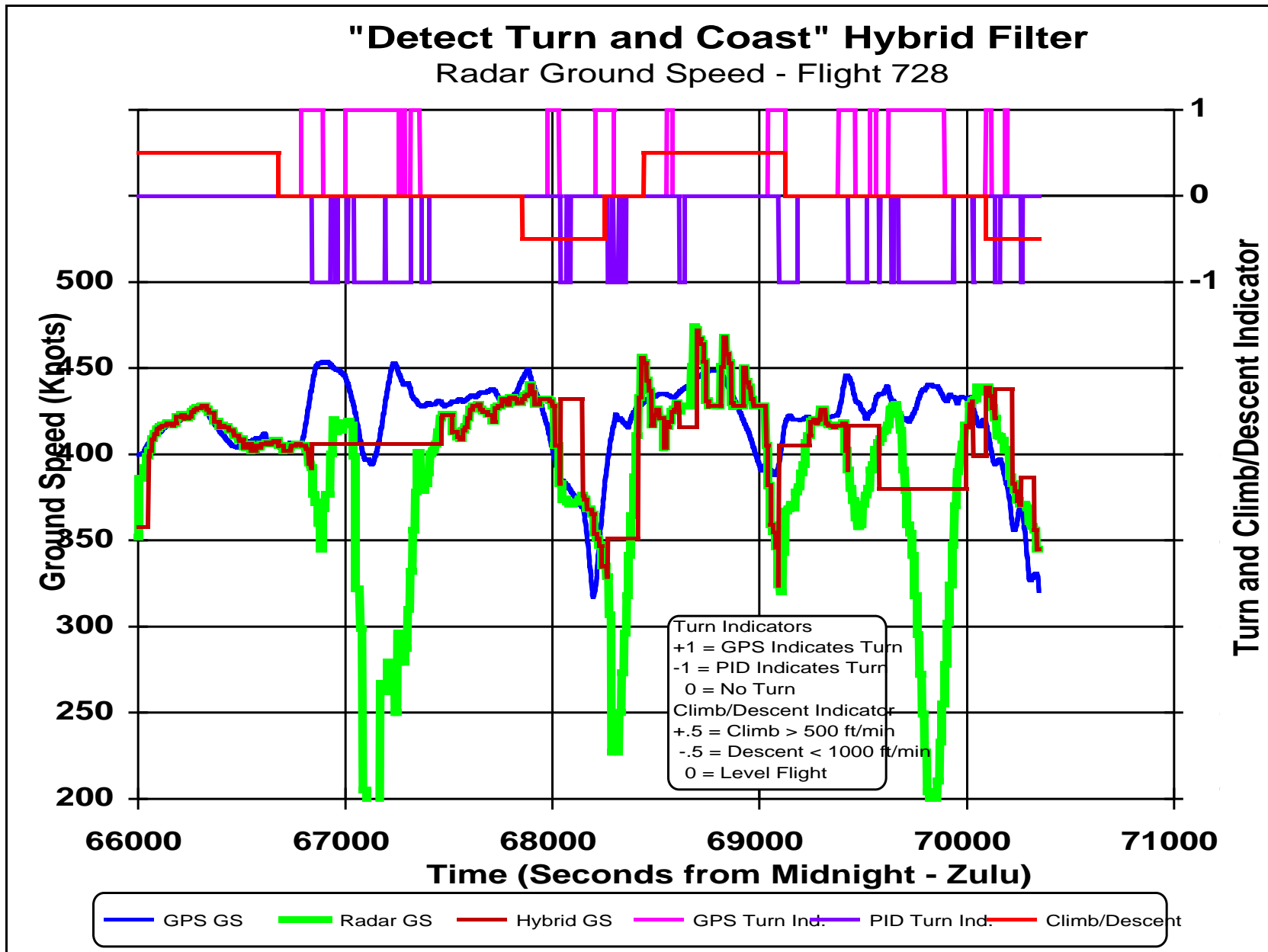


Figure 16 "Detect Turn and Coast" Hybrid Filter Using Radar Ground Speed for Second Half of Flight 728

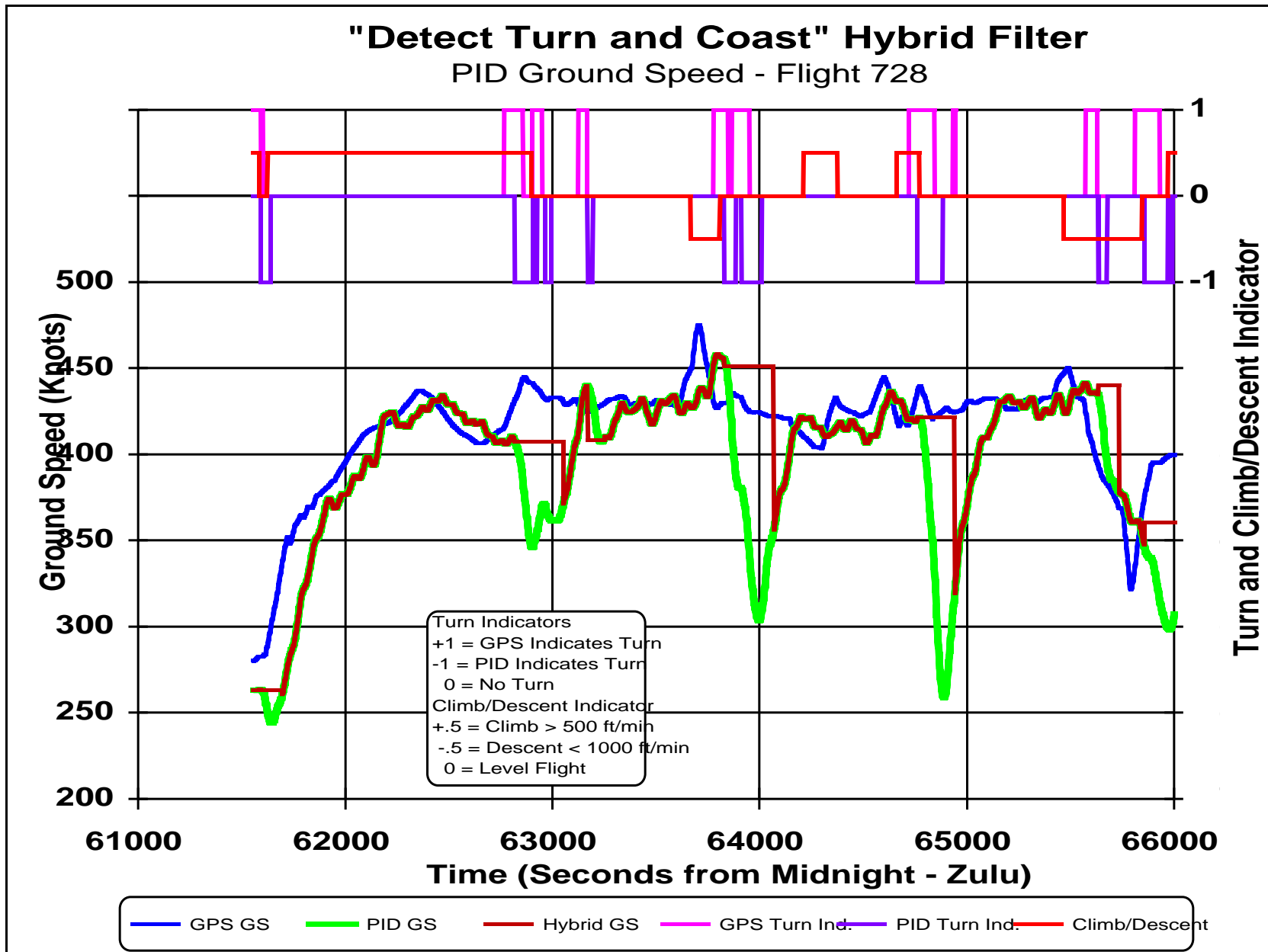


Figure 17 "Detect Turn and Coast" Hybrid Filter Using PID Ground Speed for First Half of Flight 728

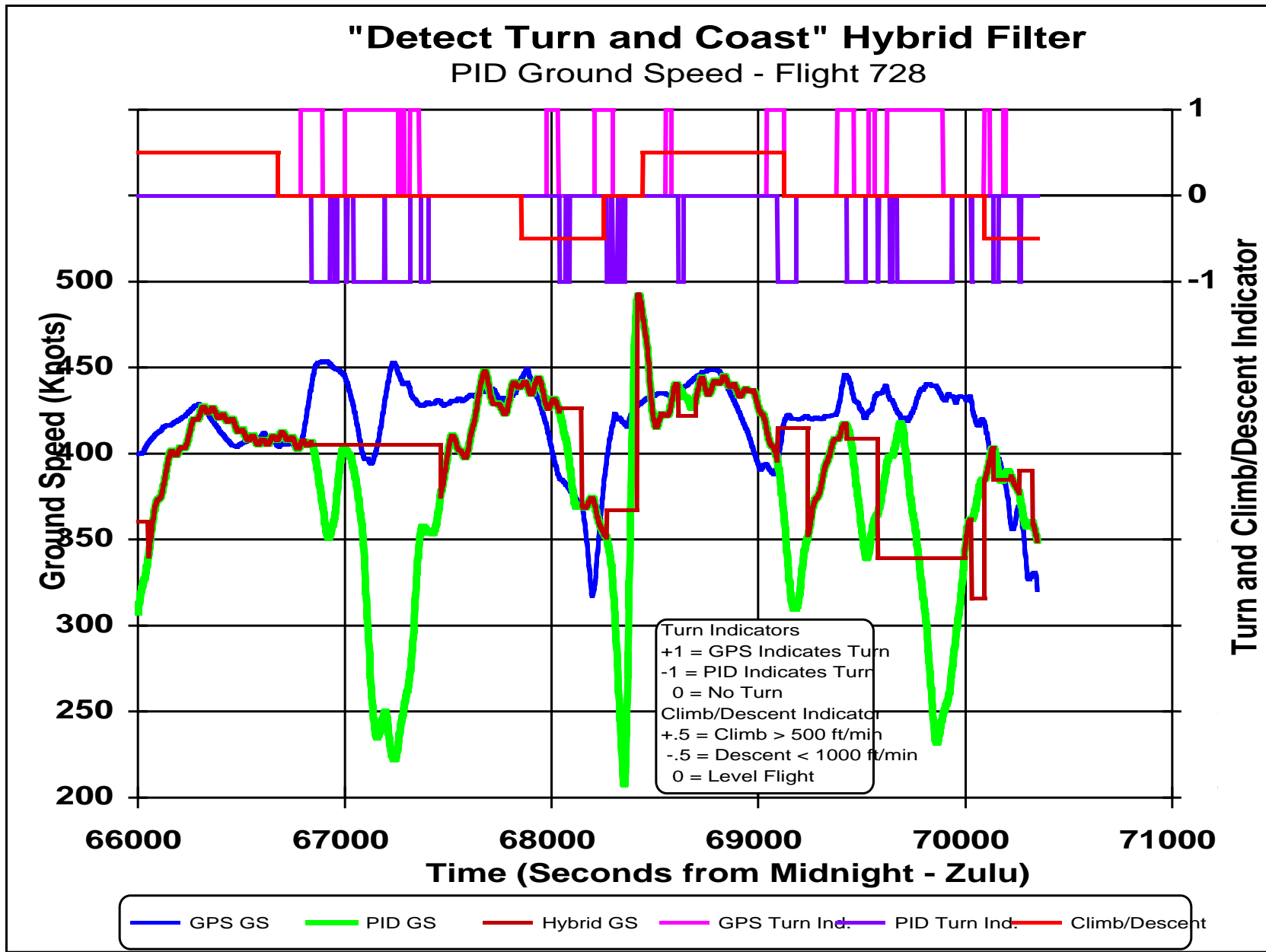


Figure 18 "Detect Turn and Coast" Hybrid Filter Using PID Ground Speed for Second Half of Flight 728

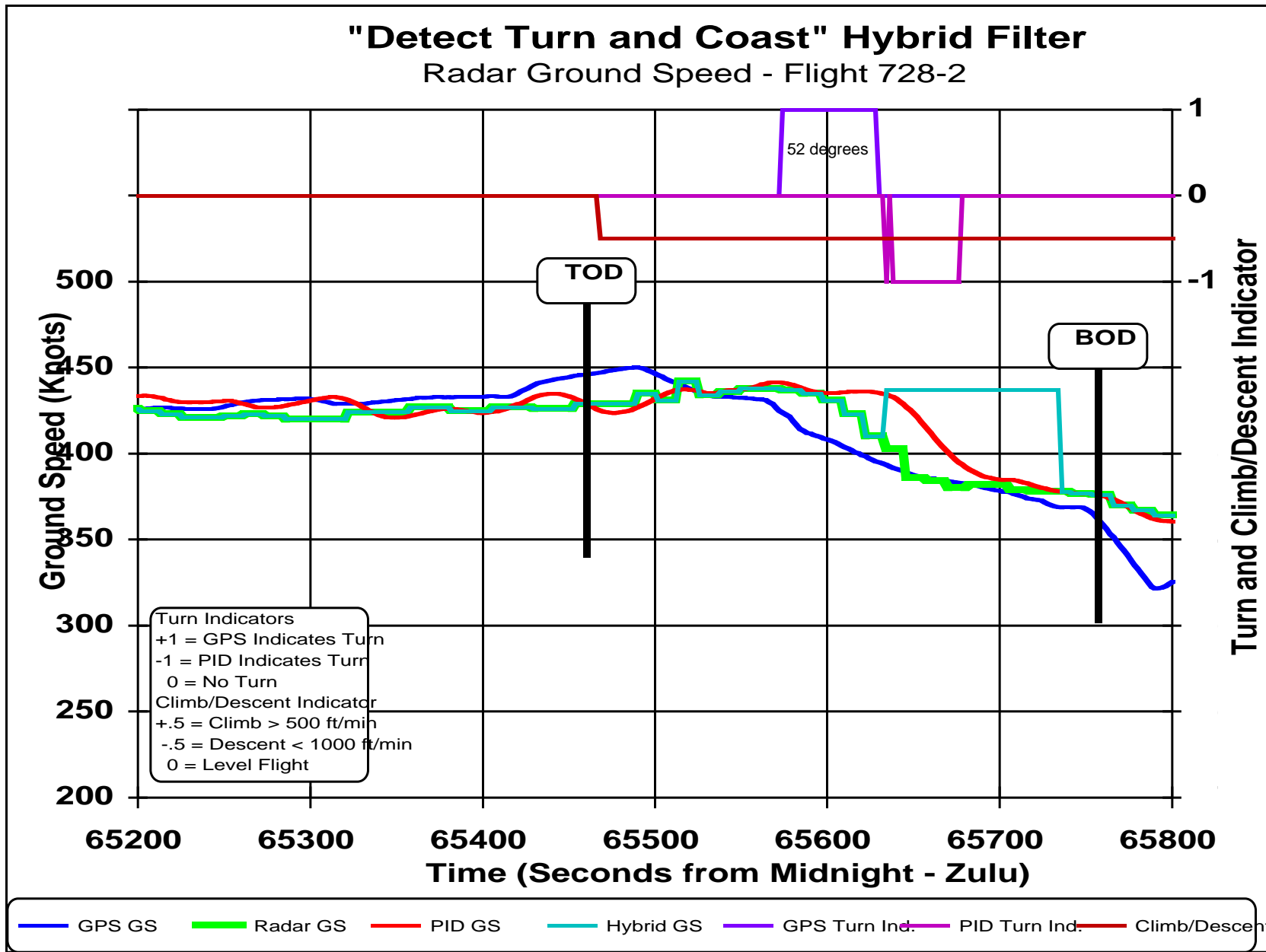


Figure 19 "Detect Turn and Coast" Hybrid Filter Using Radar Ground Speed for Flight Segment 728-2

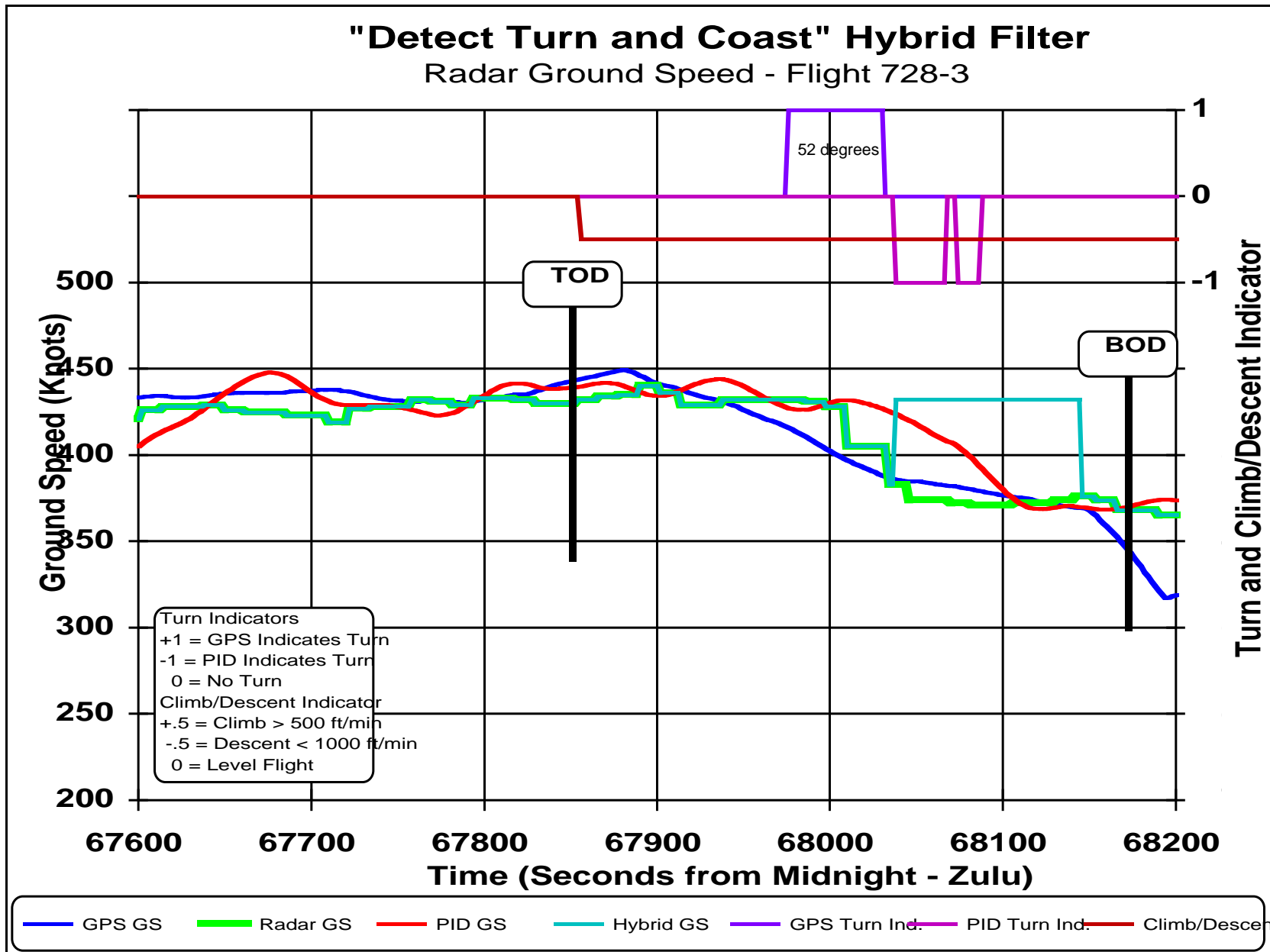


Figure 20 "Detect Turn and Coast" Hybrid Filter Using Radar Ground Speed for Flight Segment 728-3

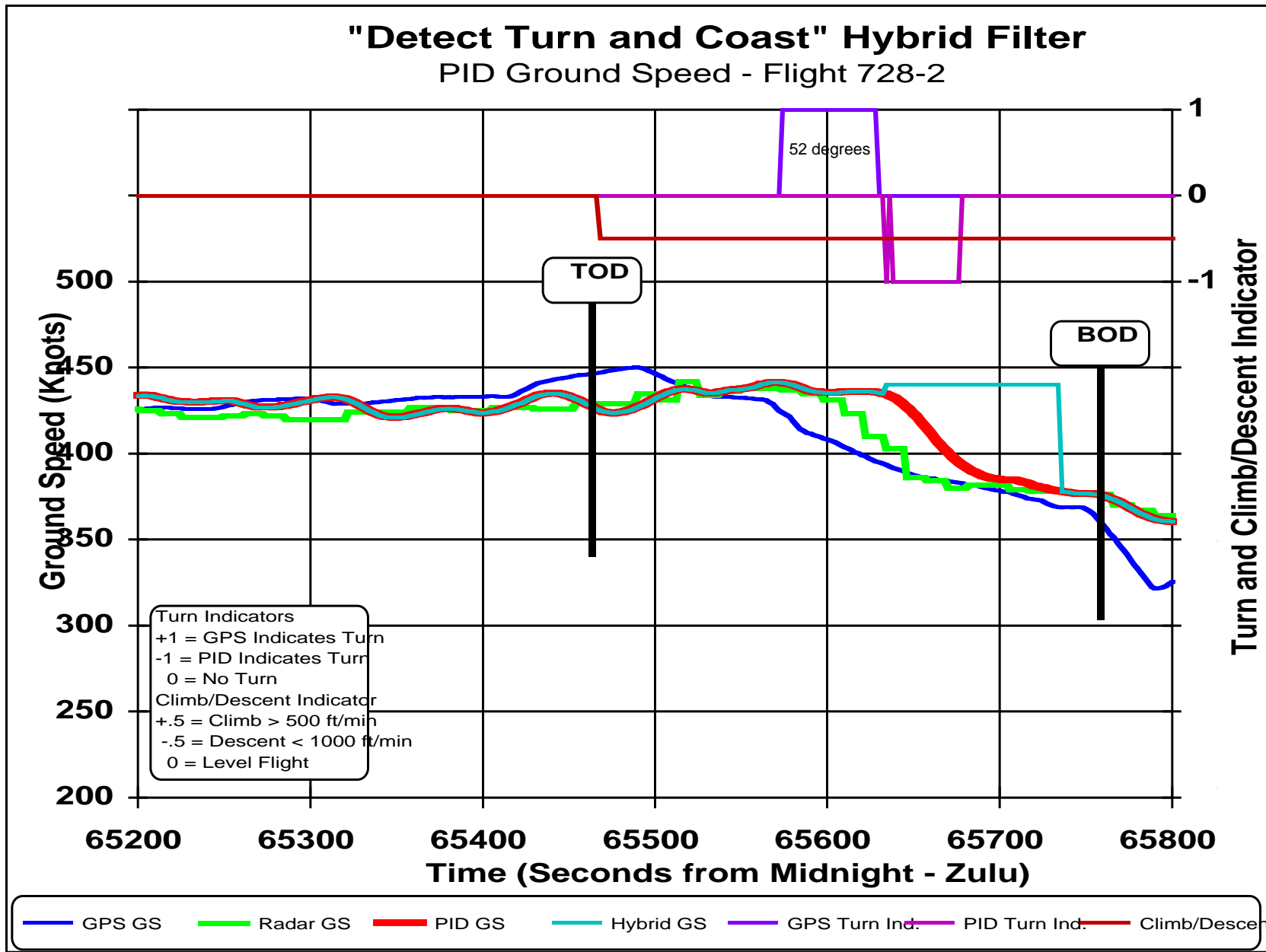


Figure 21 "Detect Turn and Coast" Hybrid Filter Using PID Ground Speed for Flight Segment 728-2

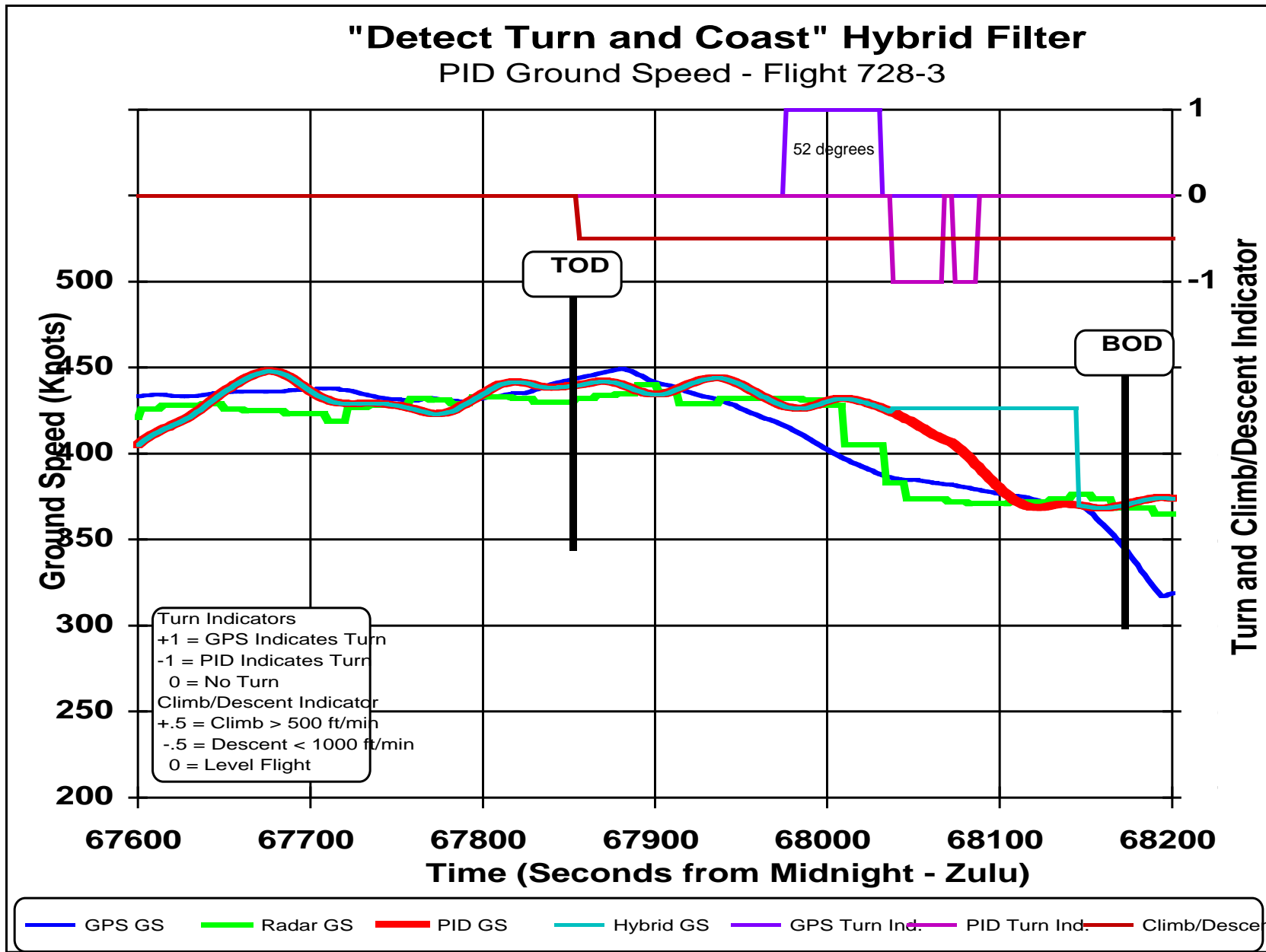


Figure 22 "Detect Turn and Coast" Hybrid Filter Using PID Ground Speed for Flight Segment 728-3

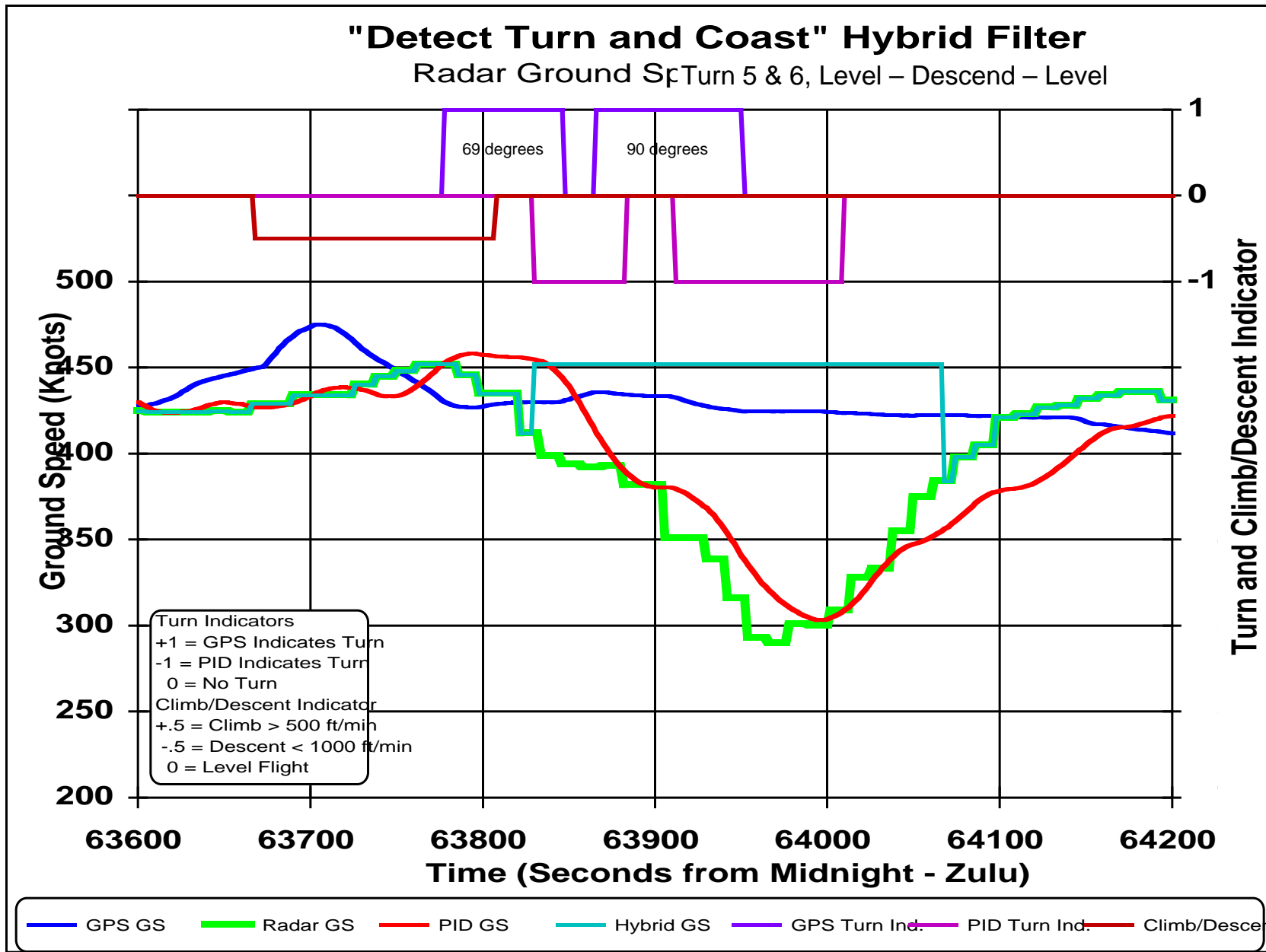


Figure 23 "Detect Turn and Coast" Hybrid Filter Using Radar Ground Speed for Flight Segment - Turn 5 and 6

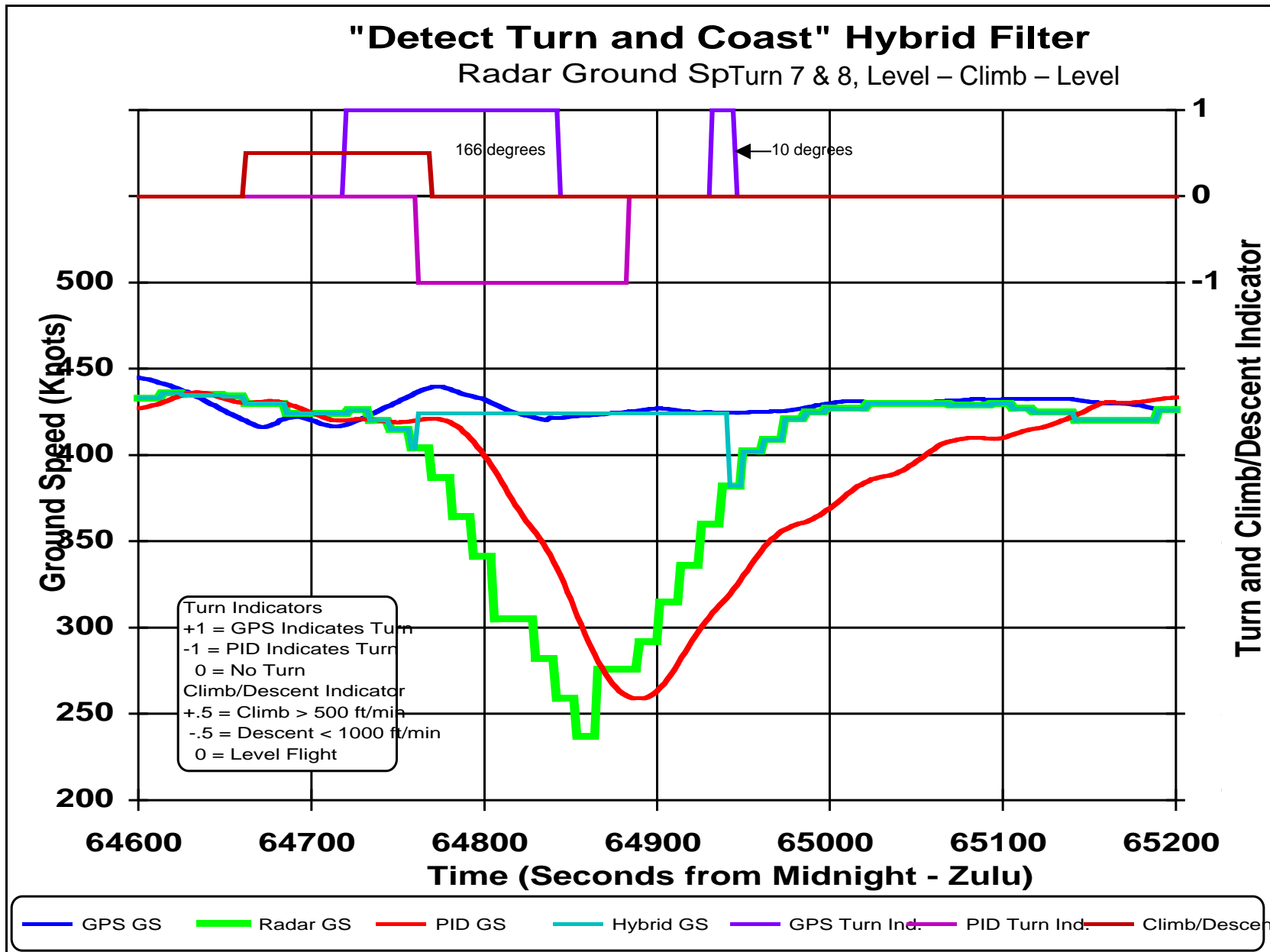


Figure 24 "Detect Turn and Coast" Hybrid Filter Using Radar Ground Speed for Flight Segment – Turn 7 and 8

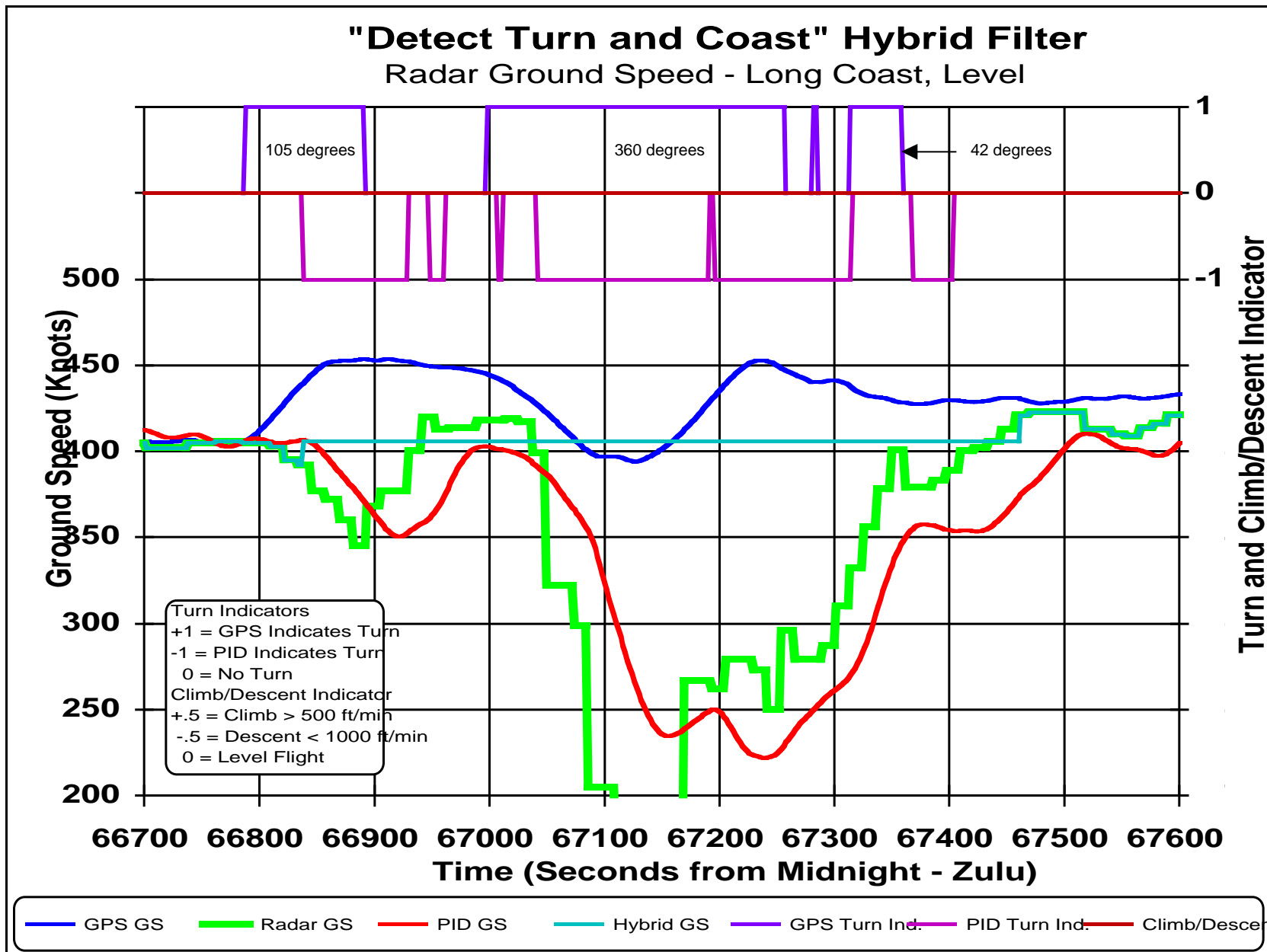


Figure 25 "Detect Turn and Coast" Hybrid Filter Using Radar Ground Speed for Flight Segment - Long Coast

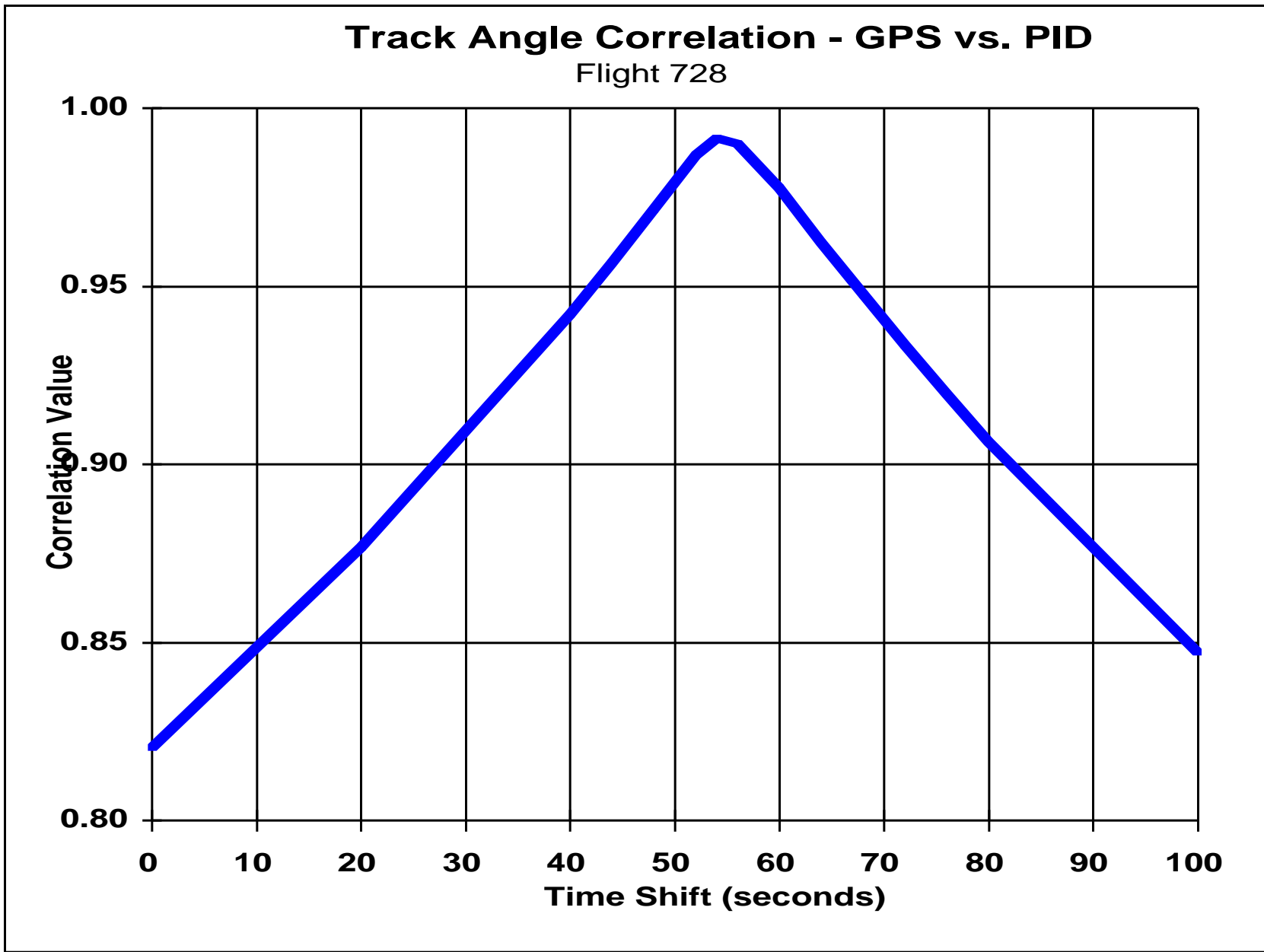


Figure 26 Correlation of GPS Track Angle and Track Angle from PID Estimator (TC = 20 seconds)

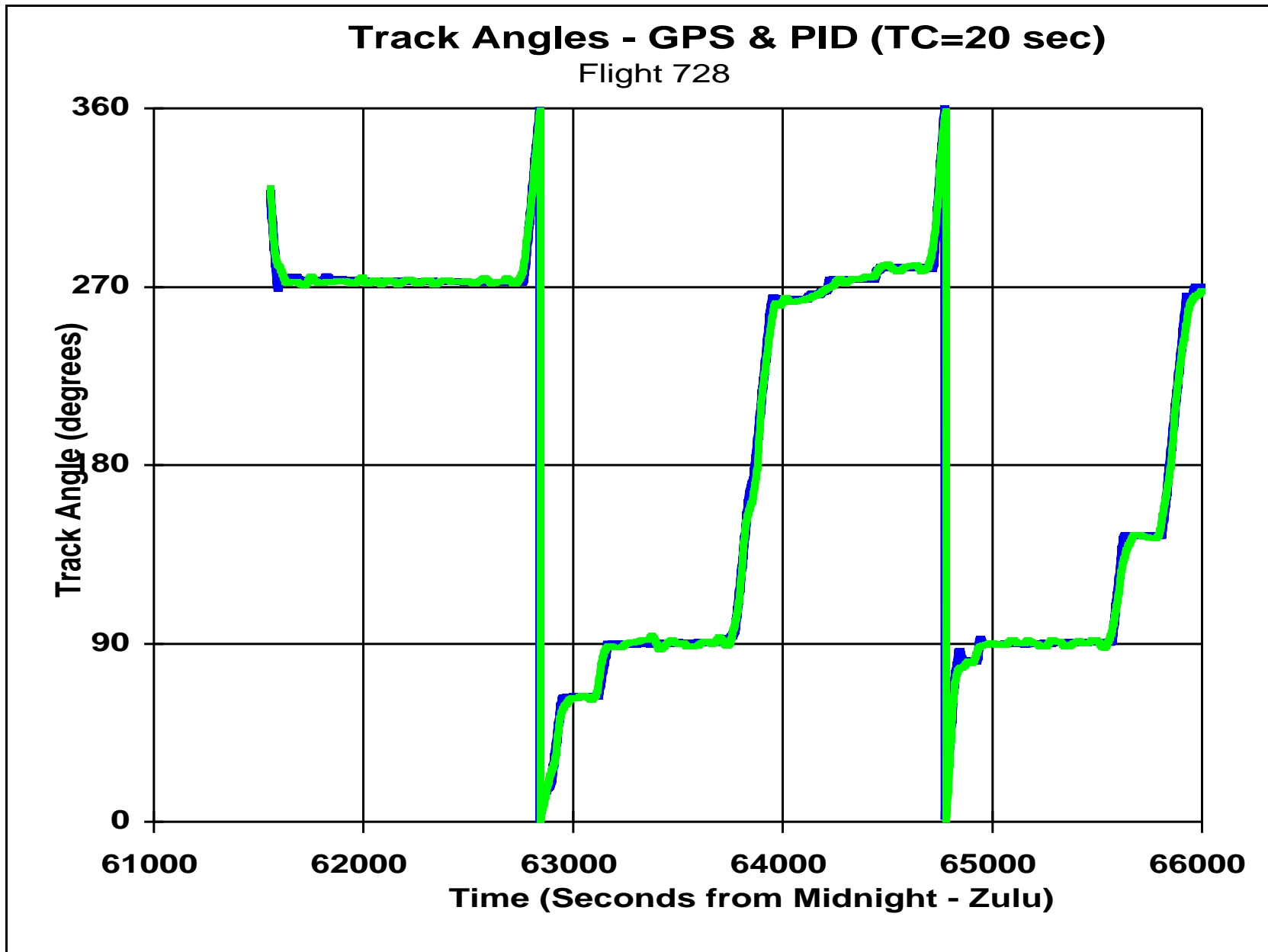


Figure 27 GPS Track Angle and Time-Shifted PID Track Angle – First Half of Flight 728

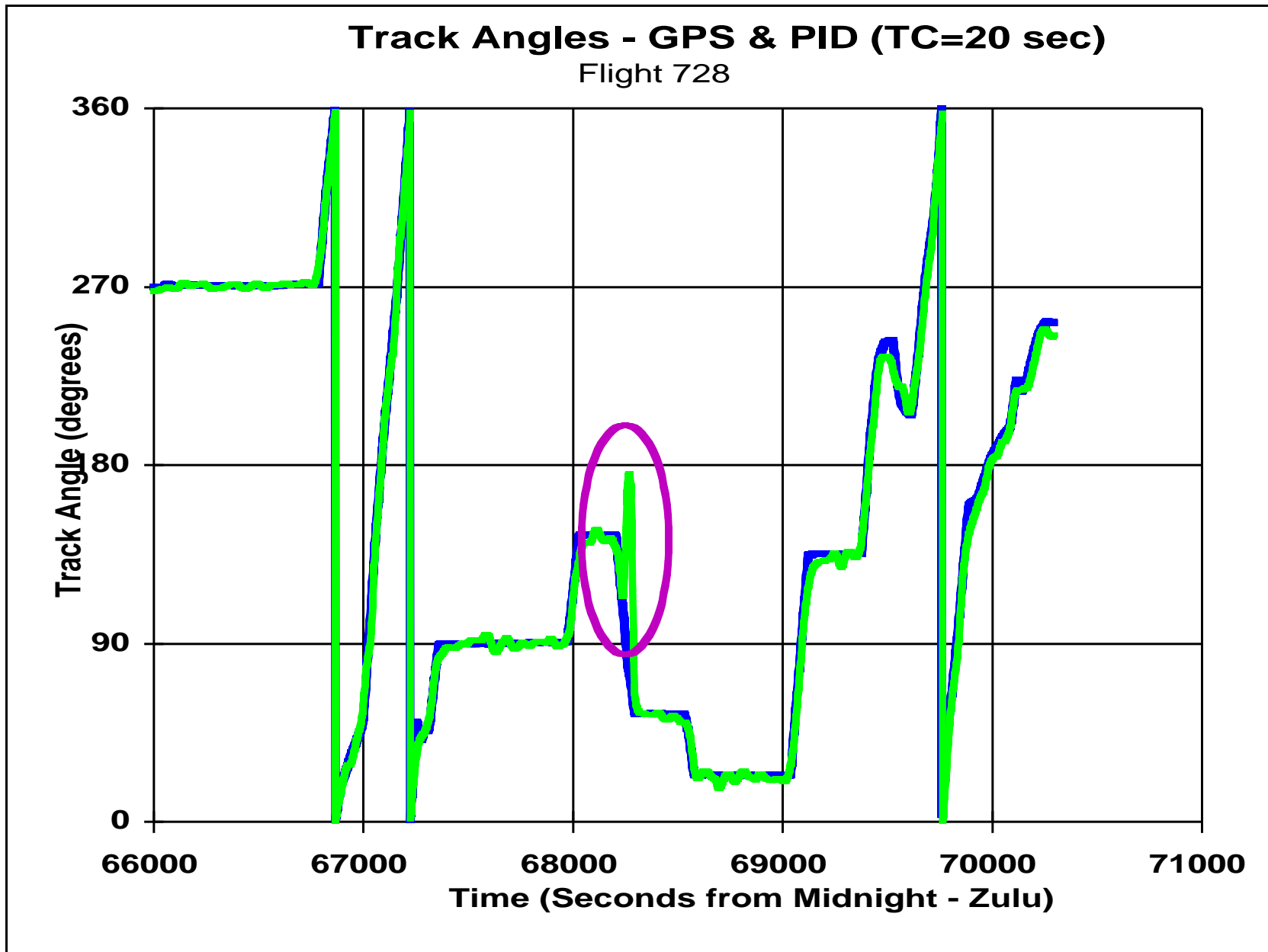


Figure 28 GPS Track Angle and Time-Shifted PID Track Angle – Second Half of Flight 728

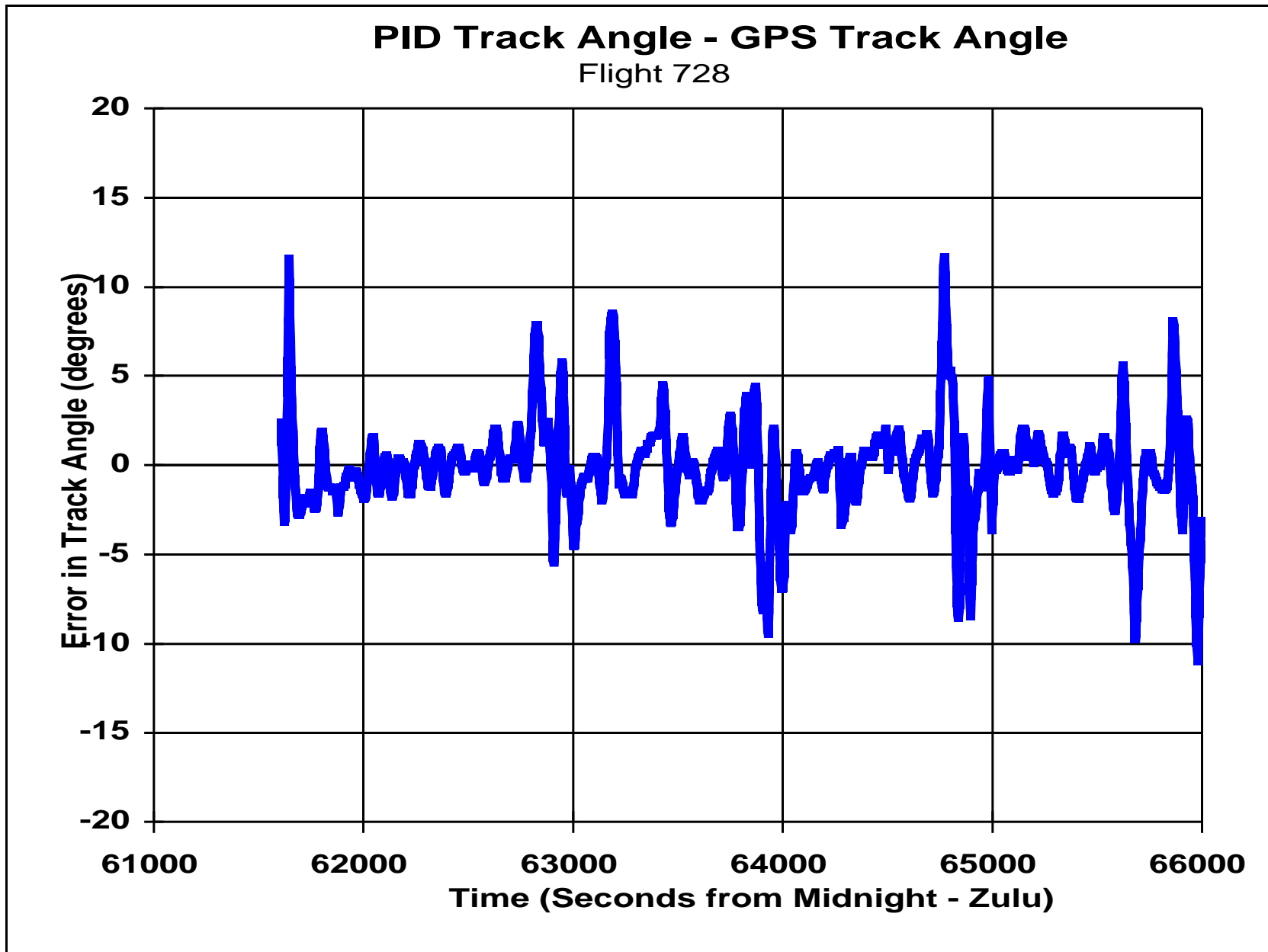


Figure 29 Error in Time-Shifted PID Track Angle – First Half of Flight 728

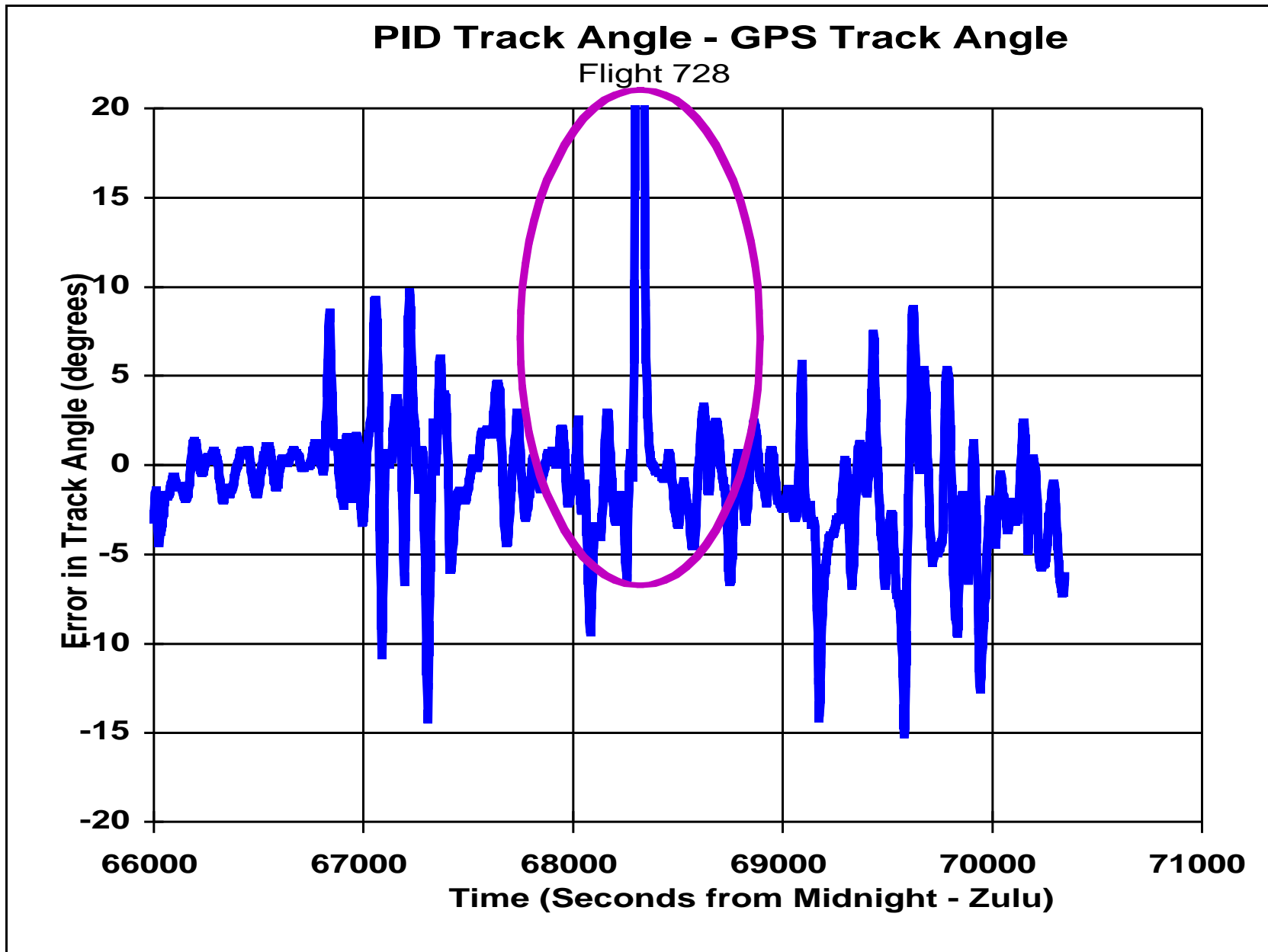


Figure 30 Error in Time-Shifted PID Track Angle – Second Half of Flight 728

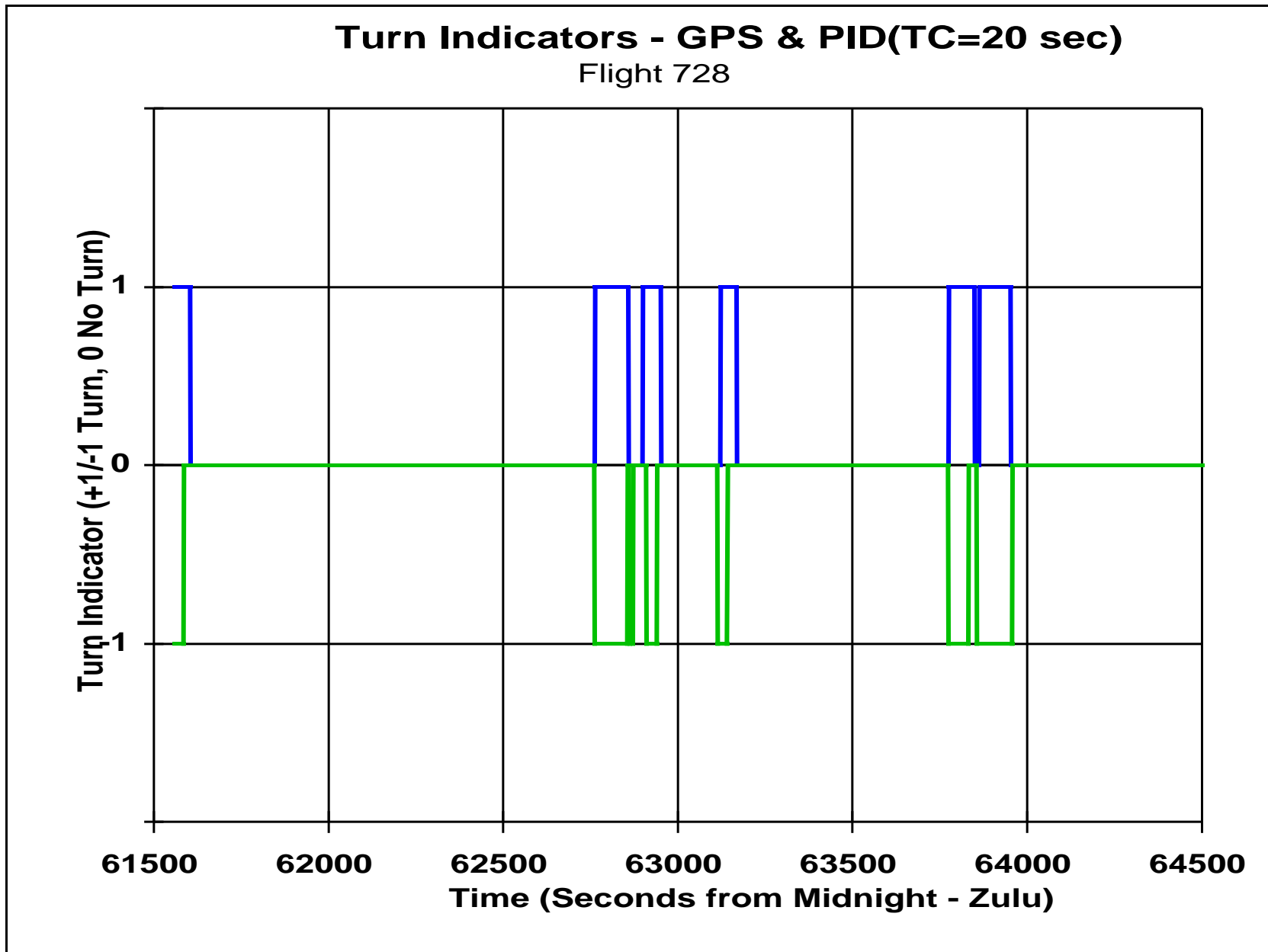


Figure 31 Comparison of GPS Turn Indicator and PID Turn Indicator for First Part of Flight 728

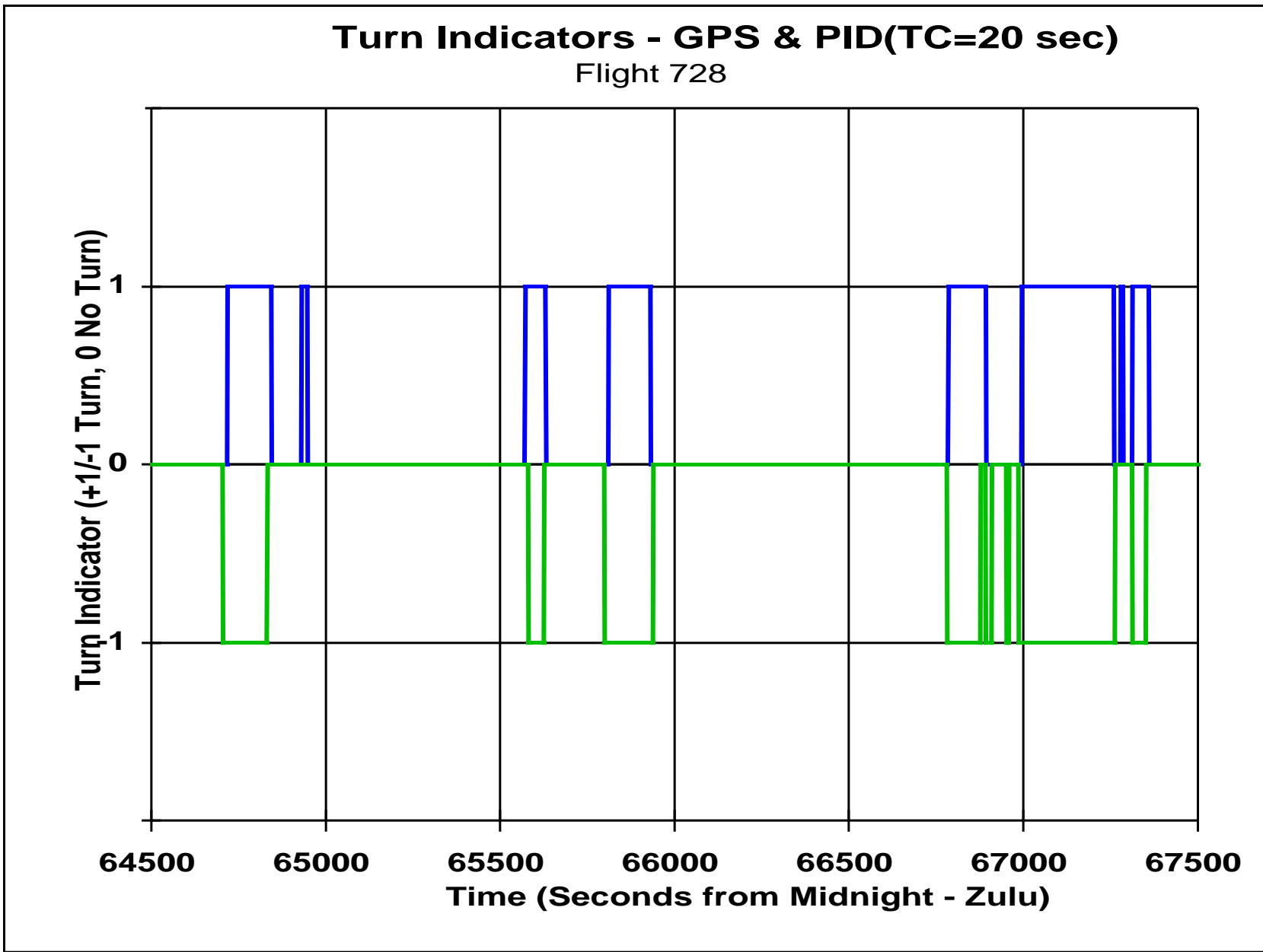


Figure 32 Comparison of GPS Turn Indicator and PID Turn Indicator for Second Part of Flight 728

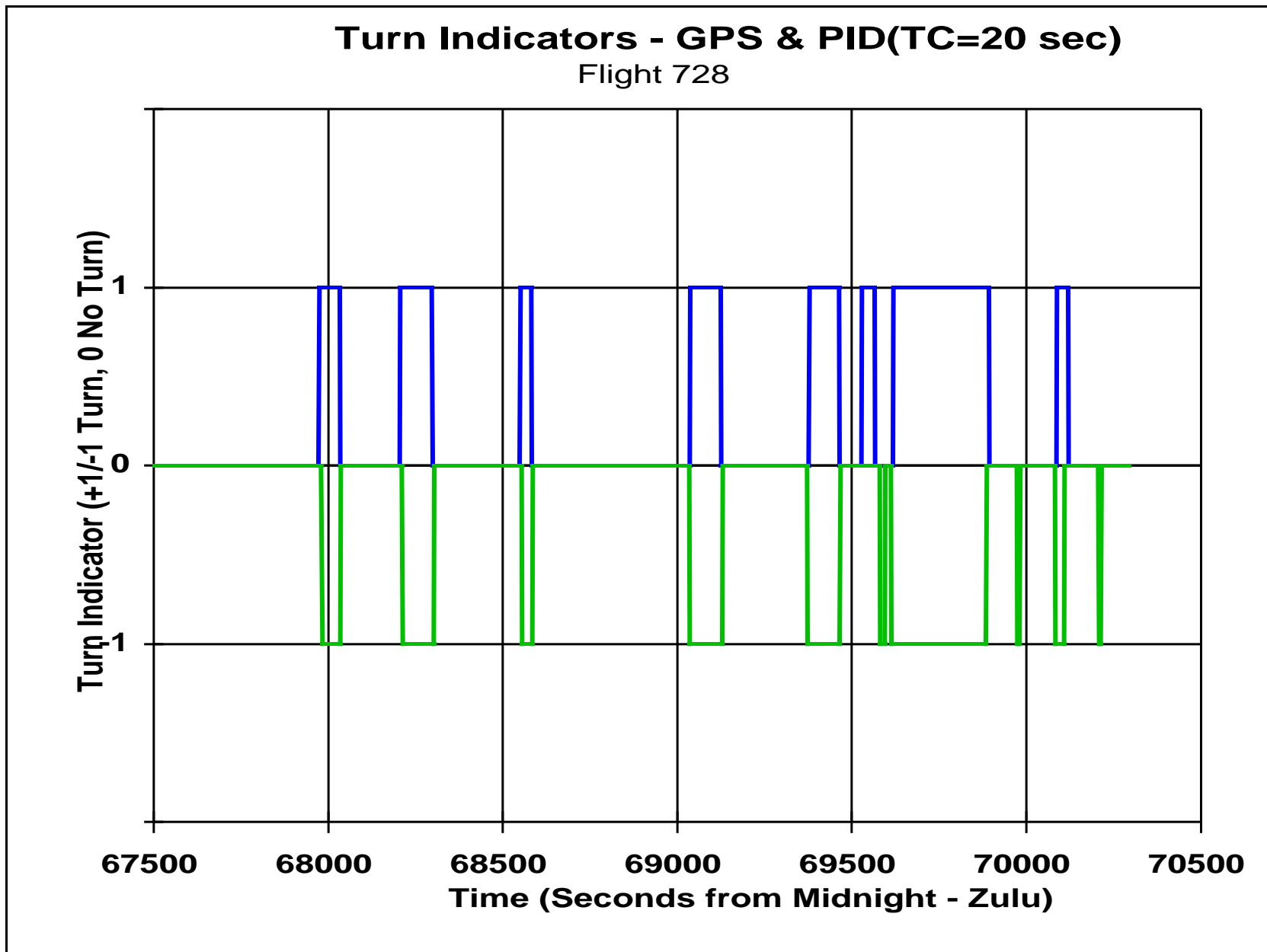


Figure 33 Comparison of GPS Turn Indicator and PID Turn Indicator for Third Part of Flight 728